U.S. DEPARTMENT OF COMMERCE
NATIONAL OCEANIC AND ATMOSPHERIC ADMINISTRATION
OCEAN PRODUCTS CENTER

TECHNICAL NOTE*

IMPLEMENTATION AND EVALUATION OF THE GULF OF ALASKA REGIONAL WAVE MODEL

Y.Y. CHAO

NATIONAL METEOROLOGICAL CENTER
WASHINGTON, D.C.
NOVEMBER 1993

---

*OPC CONTRIBUTION NO. 85

OPC CONTRIBUTIONS

No. 1. Burroughs, L. D., 1986: Development of Forecast Guidance for Santa Ana Conditions. National Weather Digest, Vol. 12 No. 1, 8pp.

No. 2. Richardson, W. S., D. J. Schwab, Y. Y. Chao, and D. M. Wright, 1986: Lake Erie Wave Height Forecasts Generated by Empirical and Dynamical Methods -- Comparison and Verification. Technical Note, 23pp.

No. 3. Auer, S. J., 1986: Determination of Errors in LFM Forecasts Surface Lows Over the Northwest Atlantic Ocean. Technical Note/NMC Office Note No. 313, 17pp.

No. 4. Rao, D. B., S. D. Steenrod, and B. V. Sanchez, 1987: A Method of Calculating the Total Flow from A Given Sea Surface Topography. NASA Technical Memorandum 87799., 19pp.

No. 5. Feit, D. M., 1986: Compendium of Marine Meteorological and Oceanographic Products of the Ocean Products Center. NOAA Technical Memorandum NWS NMC 68, 93pp.

No. 6. Auer, S. J., 1986: A Comparison of the LFM, Spectral, and ECMWF Numerical Model Forecasts of Deepening Oceanic Cyclones During One Cool Season. Technical Note/NMC Office Note No. 312, 20pp.

No. 7. Burroughs, L. D., 1987: Development of Open Fog Forecasting Regions. Technical Note/NMC Office Note. No. 323., 36pp.

No. 8. Yu, T. W., 1987: A Technique of Deducing Wind Direction from Satellite Measurements of Wind Speed. Monthly Weather Review, 115, 1929-1939.

No. 9. Auer, S. J., 1987: Five-Year Climatological Survey of the Gulf Stream System and Its Associated Rings. Journal of Geophysical Research, 92, 11,709-11,726.

No. 10. Chao, Y. Y., 1987: Forecasting Wave Conditions Affected by Currents and Bottom Topography. Technical Note, 11pp.

No. 11. Esteva, D. C., 1987: The Editing and Averaging of Altimeter Wave and Wind Data. Technical Note, 4pp.

No. 12. Feit, D. M., 1987: Forecasting Superstructure Icing for Alaskan Waters. National Weather Digest, 12, 5-10.

No. 13. Sanchez, B. V., D. B. Rao, S. D. Steenrod, 1987: Tidal Estimation in the Atlantic and Indian Oceans. Marine Geodesy, 10, 309-350.

No. 14. Gemmill, W.H., T.W. Yu, and D.M. Feit 1988: Performance of Techniques Used to Derive Ocean Surface Winds. Technical Note/NMC Office Note No. 330, 34pp.

No. 15. Gemmill, W.H., T.W. Yu, and D.M. Feit 1987: Performance Statistics of Techniques Used to Determine Ocean Surface Winds. Conference Preprint, Workshop Proceedings AES/CMOS 2nd Workshop of Operational Meteorology. Halifax, Nova Scotia., 234-243.

No. 16. Yu, T.W., 1988: A Method for Determining Equivalent Depths of the Atmospheric Boundary Layer Over the Oceans. Journal of Geophysical Research. 93, 3655-3661.

No. 17. Yu, T.W., 1987: Analysis of the Atmospheric Mixed Layer Heights Over the Oceans. Conference Preprint, Workshop Proceedings AES/CMOS 2nd Workshop of Operational Meteorology, Halifax, Nova Scotia, 2, 425-432.

No. 18. Feit, D. M., 1987: An Operational Forecast System for Superstructure Icing. Proceedings Fourth Conference Meteorology and Oceanography of the Coastal Zone. 4pp.

IMPLEMENTATION AND EVALUATION OF THE GULF OF ALASKA REGIONAL WAVE MODEL

Yung Y. Chao[1]
Development Division, National Meteorological Center

ABSTRACT

A second generation spectral wave model applicable for both deep and shallow water has been developed and implemented on a NMC CRAY-YMP computer to provide guidance forecast of wave conditions in the Gulf of Alaska. The model forecasts estimates of directional frequency spectra in 12 directional bands (30 degree/band) and 20 frequency bands (0.02Hz/band, from 0.04 to 0.42 Hz) on 30 by 30 nautical miles grids within the Gulf area extending from 155W, 53N to 132W, 61N. The model runs twice daily using wind data derived from the aviation runs of the NMC global atmospheric model forecasts. Waves are computed with a 30 minute time step to produce forecasts up to 48 hours. Model outputs for the projection hours +00, +12,+24,+36 and +48 hour are transmitted to the NWS Anchorage regional forecast office in GRIB format. The transmitted data include the combined significant wave height of both wind-sea and swell, the period and direction associated with the peak energy component of the directional spectrum, the significant wave height, mean period and mean direction of swell as well as the mean period of wind sea. The model performance has been evaluated by means of statistical error analyses using NDBC buoy wave measurements as the standard of reference and has shown that the model can provide good quality guidance forecasts.

1. INTRODUCTION

Adequate forecasts of wave conditions over the open oceans in general, and the coastal areas in particular, are required for the safety and efficiency of various recreational and industrial activities at sea.

Since the introduction of the concept of the wave spectrum in characterizing ocean surface waves in the early fifties, there has been marked progress in our understanding of the physical processes associated with wind generated waves along with improvement in computer capability. As a result, the use of numerical spectral wave models

[1]OPC Contribution No. 85

based on the energy balance equation to provide routine guidance forecasts, have become widespread at national meteorological services in many maritime countries since the last decade.

The contemporary wave prediction models can be classified as the first, second, and the third generation models (The SWAMP Group, 1985). The models differ primarily in the treatment of the nonlinear wave-wave energy transfer which, in turn, affects the forms assumed for other source terms and the choice of the numerical method to integrate the energy balance equation. In the first-generation models, the nonlinear transfer is considered to play a minor role in wave growth and is either neglected entirely or not specified explicitly. In the second-generation models, the nonlinear transfer is considered, but is not rigorously represented. Instead, the nonlinear transfer by resonant wave-wave interactions is described in terms of a few parameters, and is valid for a restricted class of spectral shapes. In the third-generation models, rigorous computation of the three-dimensional nonlinear Boltzmann intergal expression for nonlinear transfer is involved. However the computation requires substantial computer time even on a super computer, for example, the CRAY-YMP.

There are two operational spectral wave models in the United States routinely forecasting wave conditions of the global oceans including the Gulf of Alaska. One is the Fleet Numerical Oceanography Center's Global Spectral Ocean Wave Model (GSOWM), and the other is the NOAA Ocean Wave model (NOW). Both models provide 72-hour forecasts, and the spectrum is described by 15x24 discrete frequency-direction spectral components on each of about 7,000 grid points. The grid mesh is 2.5 by 2.5 degrees in latitude and longitude, extending from 70S to 75N. The major difference between the two is that GSOWM is a first generation model, while the NOW model is a second-generation model.

Questions concerning the adequacy of using these model outputs as guidance for realistic forecasts of wave conditions in the Gulf of Alaska have been raised by concerned marine forecasters. Since they are designed to predict the general wave patterns of the global-scale ocean, the output of these models cannot be accurate enough to describe small-scale, regional wave phenomena. Furthermore, these models only predict waves in deep water. Waves near the coastal areas, where most human activities are concentrated, cannot be predicted by these models. The effects of bottom conditions on wave growth, transformation and dissipation are excluded from their model formulations.

As a part of NMC's continuing effort to improve and extend wave forecasting capability over the coastal areas of the United States, a second generation regional discrete spectral ocean wave model applicable for both deep and shallow waters in the Gulf of Alaska, has been implemented. The main purpose of this report is to document the model characteristics and the results of model performance evaluation.

2. MODEL FORMULATION

The essential governing equations and computational procedures follow the model described by Golding (1983). However, numerical schemes for wave propagation and refraction follow the approach of Duffy and Atlas (1984). The model solves the energy balance equation of the form:

$$\frac{\partial E_{ij}}{\partial t} = -\nabla \cdot (\mathbf{C_g} E_{ij}) - \frac{\partial}{\partial \theta}\{(\mathbf{C_g} \cdot \nabla\theta) E_{ij}\} + S_{in} + S_{ds} + S_{nl} \tag{1}$$

where E_{ij} is the spectral density of the wave field, in a component of frequency f_i and direction θ_j, $\mathbf{C_g}$ is the group velocity, and where S_{in} represents energy input from winds, S_{ds} energy loss due to whitecapping and bottom effects and S_{nl} the redistribution of energy within the wave spectrum due to conservative nonlinear wave-wave interactions. The symbol ∇, represents the 'del' operator in the horizontal coordinates, and t, the time. The equation is solved in four stages in the following order: propagation, refraction, growth and dissipation, and nonlinear interaction. The computational method of each term is described below.

(i) Propagation

The equation to compute wave propagation is given by

$$\partial E_{ij}/\partial t = -\nabla \cdot (\mathbf{C_g} E_{ij}) \tag{2}$$

where

$$C_g = \mid \mathbf{C_g} \mid = \frac{1}{2} C \left\{ 1 + \frac{2kh}{\sinh 2kh} \right\} \tag{3}$$

and

$$C = \frac{g}{2\pi f} \tanh kh \tag{4}$$

is the phased speed. The symbols k, h, and g represent the wavenumber, water depth and gravitational acceleration, respectively.

Golding (1983) used a modified Lax-Wendroff integration scheme while Duffy and Atlas (1984) employed a scheme suggested by Takacs (1984). It is a third-order, two-step staggered grid scheme to minimize numerical dissipation and dispersion errors. For one-dimensional case, the intermediate step for the solution of the spectal density at mth grid point is given by

$$E^*_m = E^{(n)}_m - [F_{m+1/2} - F_{m-1/2}] \tag{5}$$

where

$$F_{m\pm1/2} = \mu^+_{m\pm1/2} E^{(n)}_m + \mu^-_{m\pm1/2} E^{(n)}_{m\pm1} \tag{6}$$

$$\mu^{+}_{m\pm1/2} = \left(\frac{\mu + |\mu|}{2}\right)_{m\pm1/2} \tag{7}$$

$$\mu^{-}_{m\pm1/2} = \left(\frac{\mu - |\mu|}{2}\right)_{m\pm1/2} \tag{8}$$

and where

$$\mu_{m\pm1/2} = \frac{1}{2}(C_{g_m} + C_{g_{m\pm1}})\frac{\Delta t}{\Delta \chi} \tag{9}$$

is the Courant-Friedrichs-Lewy (CFL) stability parameter. The symbols n signifies time level, Δt is the time interval, and $\Delta\chi$ is the spatial interval.

The final step gives the actual value of E at the new time step $n+1$ and is given by

$$E^{(n+1)}_m = E^{(n)}_m - [P_{m+1/2} - P_{m-1/2}]/2 + [\nu_{m+1/2}Q_{m+1/2} - \nu_{m-1/2}Q_{m-1/2}]/2 \tag{10}$$

where

$$P_{m\pm1/2} = \mu^{+}_{m\pm1/2}(E^{*}_{m\pm1} + E^{(n)}_m) + \mu^{-}_{m\pm1/2}(E^{*}_m + E^{(n)}_{m\pm1}) \tag{11}$$

$$\begin{aligned} Q_{m\pm1/2} \;=\; & [\mu^{+}_{m\pm1/2}(E^{(n)}_{m\pm1} - E^{*}_m) + \hat{\mu}^{+}_{m\pm1/2}\hat{\mu}^{+}_{m\mp1/2}(E^{*}_m - E^{(n)}_{m\mp1})] - \\ & [\mu^{-}_{m\pm1/2}(E^{(n)}_{m\pm1} - E^{*}_m) + \hat{\mu}^{-}_{m\pm1/2}\hat{\mu}^{-}_{m\pm3/2}(E^{(n)}_{m\pm2} - E^{*}_{m\pm1})] \end{aligned} \tag{12}$$

$$\hat{\mu}^{\pm}_{m\pm1/2} = (|\mu^{\pm}_{m\pm1/2}|)^{1/2} \tag{13}$$

$$\nu_{m\pm1/2} = \left(\frac{1 + |\mu|^2/\mu}{3}\right)_{m\pm1/2} \tag{14}$$

For actual two-dimensional scheme, two one-dimensional operations are applied in succession. At grid points adjacent to the coast, this scheme cannot be used because it uses values from two grid points away from the central grid. Consequently, at these points, simple upstream differencing scheme is used.

(ii) Refraction

The wave refraction effect in shoaling water of varying depth is given by

$$\frac{\partial E_{ij}}{\partial t} = -\frac{\partial}{\partial \theta}[(\mathbf{C_g} \cdot \nabla\theta)E_{ij}] \tag{15}$$

where

$$\mathbf{C_g} \cdot \nabla\theta = (\sin\theta\frac{\partial h}{\partial x} - \cos\theta\frac{\partial h}{\partial y})(\frac{2kC_g}{\sinh 2kh + 2kh}) \tag{16}$$

The direction of wave propagation, θ, is measured counterclockwise from the x-axis (positive toward east). Similar to the propagation term, the refraction term is also solved in two steps. In the intermediate step, the centered difference scheme is used to compute the derivatives for h and then the equation is solved in the flux form as

$$E_\theta^* = E_\theta^{(n)} - [F_{\theta+\Delta\theta} - F_{\theta-\Delta\theta}] \tag{17}$$

where

$$F_{\theta+\Delta\theta} = \mu^+_{\theta+\Delta\theta} E^{(n)}_\theta + \mu^-_{\theta+\Delta\theta} E^{(n)}_{\theta+\Delta\theta} \tag{18}$$

$$F_{\theta-\Delta\theta} = \mu^+_{\theta-\Delta\theta} E^{(n)}_{\theta-\Delta\theta} + \mu^-_{\theta-\Delta\theta} E^{(n)}_\theta \tag{19}$$

$$\mu^+_{\theta\pm\Delta\theta} = \left(\frac{\mu + |\mu|}{2}\right)_{\theta\pm\Delta\theta} \tag{20}$$

$$\mu^-_{\theta\pm\Delta\theta} = \left(\frac{\mu - |\mu|}{2}\right)_{\theta\pm\Delta\theta} \tag{21}$$

$$\mu_{\theta\pm\Delta\theta} = (\mathbf{C_g} \cdot \nabla\theta)_{\theta\pm\Delta\theta} \frac{\Delta t}{\Delta\theta} \tag{22}$$

At a grid point with coordinates (l, m)

$$[(\mathbf{C_g} \cdot \nabla\theta)_{\theta\pm\Delta\theta}]_{l,m} = \left[\frac{2kC_g}{\sinh 2kh + 2kh}\right]_{l,m} \cdot \left\{ \frac{[\sin(\theta \pm \Delta\theta) + \sin\theta]_{l,m}}{2} \right.$$
$$\left. \frac{(h_{l+1,m} - h_{l-1,m})}{2\Delta x} - \frac{[\cos(\theta \pm \Delta\theta) + \cos\theta]_{l,m}}{2} \frac{(h_{l,m+1} - h_{l,m-1})}{2\Delta y} \right\} \tag{23}$$

The final step then gives the actual value of E at the new time step $n+1$ as given by

$$E_\theta^{(n+1)} = E_\theta^{(n)} - [P_{\theta+\Delta\theta} - P_{\theta-\Delta\theta}]/2 + [\nu_{\theta+\Delta\theta} Q_{\theta+\Delta\theta} - \nu_{\theta-\Delta\theta} Q_{\theta-\Delta\theta}]/2 \tag{24}$$

where

$$P_{\theta+\Delta\theta} = \mu^+_{\theta+\Delta\theta}(E^*_{\theta+\Delta\theta} + E^{(n)}_\theta) + \mu^-_{\theta+\Delta\theta}(E^*_\theta + E^{(n)}_{\theta+\Delta\theta}) \tag{25}$$

$$P_{\theta-\Delta\theta} = \mu^+_{\theta-\Delta\theta}(E^*_\theta + E^{(n)}_{\theta-\Delta\theta}) + \mu^-_{\theta-\Delta\theta}(E^*_{\theta-\Delta\theta} + E^{(n)}_\theta) \tag{26}$$

$$Q_{\theta+\Delta\theta} = \mu^+_{\theta+\Delta\theta}[(E^*_{\theta+\Delta\theta} - E^*_\theta) - (E^{(n)}_\theta - E^{(n)}_{\theta-\Delta\theta})]$$
$$- \mu^-_{\theta+\Delta\theta}[(E^*_{\theta+\Delta\theta} - E^*_\theta) - (E^{(n)}_{\theta+2\Delta\theta} - E^{(n)}_{\theta+\Delta\theta})] \tag{27}$$

$$Q_{\theta-\Delta\theta} = \mu^+_{\theta-\Delta\theta}[(E^*_\theta - E^*_{\theta-\Delta\theta}) - (E^{(n)}_{\theta-\Delta\theta} - E^{(n)}_{\theta-2\Delta\theta})]$$
$$- \mu^-_{\theta-\Delta\theta}[(E^*_\theta - E^*_{\theta-\Delta\theta}) - (E^{(n)}_{\theta+\Delta\theta} - E^{(n)}_\theta)] \tag{28}$$

$$\nu_{\theta\pm\Delta\theta} = \left(\frac{1 + |\mu|}{3}\right)_{\theta\pm\Delta\theta} \tag{29}$$

(iii) Growth and Decay

The wave growth by the wind and dissipation by various mechanisms are computed simultaneously as shown by the following equation:

$$\partial E_{ij}/\partial t = S_{in} + S_{ds} \tag{30}$$

The growth of waves is determined according to conventional linear and exponential terms representing, respectively, an excitation by turbulence fluctuation in the surface wind and the coupling of existing waves with mean shear flow in the marine boundary layer as given by

$$S_{in}(f,\theta) = \alpha + \beta E(f,\theta) \tag{31}$$

The linear term, α, is given by

$$\alpha = \begin{cases} \alpha_1 U^2 \cos^2(\theta - \psi) & \text{for } f = f_{max},\ |\theta - \psi| < 90^\circ \\ 0 & \text{otherwise} \end{cases} \tag{32}$$

where

$$\alpha_1 = 6.87 \times 10^{-8}/(2\pi f_{max}) \tag{33}$$

U is the wind speed at a 10 meter height above the mean sea surface, ψ the wind direction and f_{max} is the highest frequency component specified in the model. The β term is given, according to Snyder et al. (1981), by

$$\beta = \begin{cases} \beta_1 f \left[\frac{U\cos(\theta-\psi)}{C} - 1\right] & \text{if } U\cos(\theta-\psi)/C > 1 \\ 0 & \text{otherwise} \end{cases} \tag{34}$$

where

$$\beta_1 = 6 \times 10^{-2} \times 2\pi\rho_a/\rho_w \approx 0.37 \times 10^{-3} \tag{35}$$

and where ρ_a and ρ_w are densities of air and water, respectively.

The energy dissipation term consists of whitecapping, bottom friction and bottom percolation, i.e.,

$$S_{ds} = D_w + D_f + D_p \tag{36}$$

The energy dissipation caused by whitecapping, D_w, is given as

$$D_w(f,\theta) = -4 \times 10^{-4} f^2 E(f,\theta) \left\{ \int\int E(f,\theta) d\theta df \right\}^{1/4} \tag{37}$$

which is a modified version of the form originally suggested by Hasselemann (1974). Since the present form does not exactly balance the input energy from the wind when a fully developed spectrum was reached, the following condition is imposed:

$$0 \le (\bar{S}_{in} + \bar{D}_w)\,\Delta t + \bar{E}_w < \bar{E}_{pm} \tag{38}$$

where the overbar represents integration over frequency and direction. $\bar{E}_{pm}$ is equivalent to the total energy of Pierson-Moskowitz fully developed spectrum (Pierson and Moskowitz, 1964) as given by

$$\bar{E}_{pm} = ag^2(2\pi f_{pm})^{-4}/5 \approx 3.594 \times 10^{-3} U^4 g^{-2} \tag{39}$$

with $a = 8.1 \times 10^{-3}$. The term f_{pm} is originally given at a height of 19.5 meter and is approximate to a 10 meter height by using the relation $0.0397U_{19.5} = 0.0425U$ so as

$$f_{pm} = 0.1396g/U_{19.5} = 0.1304g/U \tag{40}$$

The term $\bar{E}_w$ is the total energy in the wind-sea part of the spectrum as given by

$$\bar{E}_w = \int_{\theta-\psi=-90^\circ}^{\theta-\psi=90^\circ} \int_{f_{min}}^{\infty} E(f,\theta) df d\theta \tag{41}$$

where $f_{min} = 0.8 f_p$ and $f_p$is the frequency of peak energy (to be defined later).

The energy dissipation due to bottom friction is calculated by using the approximate form of Collins (1972):

$$D_f = \frac{-c_f g k^2 |C_g|}{(2\pi f \cosh kh)^2} \langle u \rangle E(f,\theta) \tag{42}$$

where the friction factor $c_f = 0.05$ and

$$\langle u \rangle = \left\{ \int\int (gk/2\pi f \cosh kh)^2 E(f,\theta) df d\theta \right\}^{1/2} \tag{43}$$

The energy loss due to bottom percolation is based on Shemdin et al. (1980):

$$D_p = -\sqrt{c_h c_v} k E(k,\theta) \tanh\{\sqrt{c_h/c_v} kd\} / \cosh 2kh \tag{44}$$

where d is the depth of sand layer, and c_h and c_v are the horizontal and the vertical permeability coefficients, respectively. Using laboratory results, Sleath (1970) suggested coefficients of permeability for a coarse sand (mean diameter 1.3 mm, standard deviation 0.46 mm) to be $c_h = 1.26, c_v = 0.89$ and for a fine sand (mean diameter 0.38 mm, standard deviation 0.10 mm) to be $c_h = 0.145, c_v = 0.126$. For an isotropic sand, $c_h = c_v$, with a deep sand layer in which $d > 0.3 \times wavelength$, the equation simplifies to

$$D_p = -c_h k E(f,\theta) / \cosh^2 kh \tag{45}$$

The damping rates are in the order of $10^{-3}/sec$ for coarse sand and $10^{-4}/sec$ for fine sand. The algorithm for energy loss due to percolation is available in the computer program, but is not executed at present.

(iv) Nonlinear Interactions

The nonlinear wave-wave energy transfer is considered in a parameterized and rather empirical manner. It is based on the assumption that nonlinear interaction will always act to bring the wind-sea spectrum back to the following modified JONSWAP (Joint North Sea Waves Project) spectrum (Hasselmann et al., 1973). The shape equation is defined as

$$E_{JT}(f,\theta) = F_T(f)\exp\left\{-1.25\left(\frac{f_p}{f}\right)^4 + \ln\gamma\exp[\frac{-(f-f_p)^2}{2\sigma^2 f_p^2}]\right\}G(f,\theta) \tag{46}$$

where the angular spreading function $G(f,\theta)$ is given by

$$G(f,\theta) \propto \begin{cases} \cos^2(\theta-\psi) & \text{for } \mid \theta-\psi \mid < 90^\circ \\ 0 & \text{otherwise} \end{cases} \tag{47}$$

and where $F_T(f)$ is the saturation range in water of arbitrary depth suggested by Thornton (1977):

$$F_T(f) = \kappa C^2(f) f^{-3} \tag{48}$$

where κ is adjusted to conserve the total wind-sea energy.

The peak frequency f_p of the wind-sea spectrum which is unknown a priori is determined in the following manner. First, the peak frequency is approximated as the peak frequency of P-M spectrum, i.e., $f_p = f_{pm}$. The total wind-sea energy $\bar{E_w}$ is then calculated according to the definition given previously with $f_{min} = 0.8 f_p$. A new f_p is calculated by an approximate relation of form

$$f_p = (2.5\times 10^{-4}/\bar{E}_w)^{1/4} \approx 0.1\bar{E}_w^{-1/4} \tag{49}$$

With this f_p the total energy of wind-sea, $\bar{E_w}$ is recalculated. The final peak frequency value along with the peak enhancement of the modified JONSWAP spectrum are calculated using formulae which approximate to the single-parameter model of Hasselmann et al. (1976).

$$f_p = \{[2.5\times 10^{-4} + 7.4\times 10^{-4}(\gamma-1)\sigma]/\bar{E}_w\}^{1/4} \tag{50}$$

$$\gamma = 1.0 + 2.3[1-(\bar{E}_w/\bar{E}_{pm})^2] \tag{51}$$

Using these parameters and the peak width $\sigma = 0.08$, the shape spectrum, E_{JT}, is evaluated and is used to replace the spectral components in the wind-sea part of the spectrum.

3. FORECAST PROCEDURES, INPUTS AND OUTPUTS

The Gulf of Alaska regional wave model (GAK) forecasts estimates of directional frequency spectra in 12 directional bands (30 degree/band) and 20 frequency bands(0.02

Hz/band, from 0.04 Hz to 0.42 Hz) at each grid point in the Gulf area extending from 155W, 53N to 132W, 61N (see Figure 1). A domain with a grid size of 30 by 30 nautical miles is established for the gulf region. A total of 30x18=540 grid points is involved. The wave model runs twice daily on NMC CRAY-YMP for 0000 UTC and 1200 UTC. Waves are computed with a 30 minute time step to produce forecasts up to 48 hours.

To predict wave conditions for the areas of interest in the Gulf, it is necessary to consider waves both propagating in from the Pacific and those generated by local winds, as well as the effects of bottom topography on waves. The depth value at each grid point is digitized from a bathymetric chart. Each computer run of the model begins with acquiring analyzed and forecast wind data from the NMC's Global Data Assimilation System (GDAS) and Aviation (AVN) runs of the global atmospheric spectral model (Kanamitsu, et al., 1991; Parrish and Derber, 1992). From the model one obtains winds with a horizontal grid resolution of $1^\circ \times 1^\circ$ in latitude/longitude.

The lowest sigma layer of the global atmospheric model has a thickness of 10 mb. Hence the computed winds in the lowest layer correspond to a height of about 50 m above the mean sea level and it is necessary to reduce these winds to a height of 10 m height above the sea surface for the wave model. A logarithmic wind profile is assumed for computations. Furthermore, as the final step in preparing the surface wind fields for the wave model, the surface wind data which are given on $1^\circ \times 1^\circ$ resolutions, are interpolated to 30 by 30 nm wave model grids.

In order to account for waves entering the Gulf region from the Pacific Ocean, wave information on the outer edge of the Gulf, i.e., in the boundary zone of the Gulf region and the open ocean, must be provided routinely. The boundary values for the GAK model are derived from the operational global wave model, NOW. As mentioned earlier, the model has a grid mesh of 2.5 by 2.5 degree in latitude and longitude extending from 70S to 75N. It provides wave spectral information at every 3 hour time step from -12 h up to 72 h. Hindcast and forecast spectra at each global grid point in the boundary zone are interpolated to regional grid points in the boundary zone. A linear weight function is used to calculate the global-regional combined spectrum in the boundary zone such that a smooth transition from the 100 % global wave data at the outer-most grids to the 100% regional wave data at inner-most grids is achieved.

In order to determine initial wave conditions for each cycle run, a wave hindcast is made prior to wave forecasting by using analyzed wind fields at -12 h, -06 h and +00 h. Wave hindcasts are computed with analyzed wind data and the final hindcast wave field of the previous cycle run as initial values. The hindcast wave field at +00 h then serves as the initial wave condition for wave forecasting through the present cycle run as well as the initial wave condition for the next cycle wave hindcast. It should be noted that the same hindcasting procedure is also used for the global wave model.

A schematic representation of the flow of wind and wave forecasting procedures described above is given in Figure 2. The outputs from GAK model include:

1. The significant wave height, peak energy direction and period of wind-sea and swell combined for all grid points at 0, +12, +24, +36 and +48 hr.

2. The significant wave height, mean period and direction of swell for all grid points at 0, +12, +24, +36 and +48 hr.

3. The significant wave height, mean period and direction of wind sea for all grid points at 0, +12, +24, +36 and +48 hr.

4. Directional spectra and the above wave parameters at selected grid points at 3 hr. intervals for verification and/or providing input boundary conditions for the site specific local wave models.

5. Directional spectra at all grid points at 00 h to provide initial data for next cycle run.

Among them, items 1, 2, and the mean period of the wind sea for the projection hours +00, +12, +24,+36 and +48 hour are packed into the WMO (World Meteorological Organization) GRIB (GRIdded Binary) code and transmitted to NWS Anchorage regional forecast office through a high speed telecommunication line.

4. FORECAST PERFORMANCE EVALUATION

Buoy Data

As shown in Figure 1, there are several data buoys which have been deployed in the Gulf of Alaska. Buoys No. 46001 and No.46003 are operated by the NOAA Data Buoy Center (NDBC), while the rest belongs to Canadian Atmospheric Environment Service, Marine Data Unit. Wind and wave data were acquired from these buoy measurements during the period April 1, 1993 through September 30, 1993. From Buoy 46001, which is located near the center of the Gulf (56.3N, 148.2W), about 80% of the expected complete data set has been obtained while less than 30% are retrieved from the rest. These buoys have either been in maintenance or in repair for most of this time period. The present statistical evaluation of the GAK model performance, therefore, is made mainly from data obtained at Buoy 46001.

Both buoys 46001 and 46003 are of 6-meter NOMAD hull type. NOMAD has an anemometer at a 5 meter height, an axial linear accelerometer, and a Data Acquisition Control and Telemetry (DACT) payload including the so-called Wave Analyzer (WA) wave data processing system. The WA system provides spectral estimates with 0.01 Hz bandwidth and 24 degrees of freedom based on hourly 20 min long records sampled at 2 Hz. The upper and lower bounds of the 90% confidence interval are, respectively, 1.52 and 0.58 of the estimated value. The DACT relays encoded wave data and meteorological data such as wind speeds and directions to NMC via the Geostationary Operational Environmental Satellite (GOES). The frequency bands of the reported frequency spectra range from 0.03 to 0.40 Hz (Steel et al., 1986; Steele et al., 1992).

Wave Heights and Winds

A statistical error analysis was performed for the significant wave height model output by using buoy measurements as the standard of reference. For GAK, wave heights are taken from the grid point nearest to the buoy location. For the global wave model, wave heights are determined by interpolating the values from the surrounding four grids.

Since no single statistical index can provide the complete description of model performance, a series of statistical indices were calculated for this study. The indices consisted of the mean bias error $BIAS$, root mean square error RMS, correlation coefficient CR and scatter index SI. A least squares regression analysis was also made to determine the best fit linear equation of the scatter diagram. These indices take the forms

$$BIAS = \frac{1}{N}\Sigma(P_i - O_i), \tag{52}$$

$$RMS = \left\{\frac{1}{N}\Sigma(P_i - O_i)\right\}^{1/2}, \tag{53}$$

$$CR = \frac{\Sigma[(P_i - \bar{P})(O_i - \bar{O})]}{\{\Sigma(P_i - \bar{P})^2\Sigma(O_i - \bar{O})^2\}^{1/2}}, \tag{54}$$

and

$$SI = RMS/\bar{O}, \tag{55}$$

where N is the number of data points, and $\bar{P}$ and $\bar{O}$ are the means values of model predictions, P_i, and measurements, O_i, respectively. The simple linear least squares regression curve is given by

$$y = ax + b \tag{56}$$

where x and y represent measured and predicted variables, and

$$a = \frac{\Sigma[(P_i - \bar{P})(O_i - \bar{O})]}{\Sigma(O_i - \bar{O})^2} \tag{57}$$

$$b = \bar{P} - a\bar{O} \tag{58}$$

The accuracy of wave model forecast is strongly affected by the accuracy of the forecast wind, initial wind and wave conditions as well as input wave data from the global wave model, NOW, in the boundary zone. In Figure 3, initial wind and wave conditions used in the wave model (for +00 h) are shown. In general, the estimated wind speeds have a tendency to being slightly higher than measured values. However, a root mean square error of less than 2 m/s, and a correlation coefficient of as high as 0.93 indicate that the analysis procedure is adequate. The initial wave conditions which are hindcast products of analyzed wind field alone, are slightly higher than measurements and are consistent with the trend of analyzed wind speeds. The resulting wave height error, however, is acceptable.

Figure 4 shows scatter diagrams of forecast and measured significant wave heights at +12, +24, +36, and +48 h. As expected, the longer the projection hour, the lower the model performance. However, on the average, the values of bias 0.26 m, root mean square error 0.65 m, correlation coefficient 0.85 and scatter index 30% are quite reasonable.

Figures 5(a) and 5(b) show scatter diagrams for the wind speed and the wind direction, respectively, at the same projection hours as given in Figure 4. As shown in Figure 5(a), the correlation between forecast and measured wind speeds is not quite satisfactory, the average correlation coefficient value is 0.72. At +48 h, the value drops to only 0.63. In contrast, as shown in Figure 5(b) in which the minus sign indicates that the angle is measured counterclockwise from north, the forecast wind direction agrees better with the measurement. Though there is a certain increase in the amount of deviation of model forecasts from measurements as the projection time increase, the trend is not as strong as that of the wind speed. The mean RMS error in the wind direction is 35 degree. The maximum is 48 degree at +48 h. These results indicate that the global atmospheric model may not be able to forecast adequately the wind speed over the Gulf. It is well known that the wind condition in the Gulf of Alaska is quite complex due to the effects of existing steep mountains and extensive glaciers along the coast. A regional wind model capable of taking this special orographic influence into account may be necessary.

Figure 6 shows the results of statistical analysis at buoy 46001 for the global wave model NOW. In comparison with Figure 3, it is obvious that the performance by the NOW model is not as good as the regional model.

Wave Spectra

It is worthwhile to examine if the wave model can describe adequately the behavior of spectral evolution during the processes of growth and decay as well as during the co-existence of both wind wave and swell. The following examples are intended to address this concern.

Figures 7(a) and 7(b) show model and measured frequency spectra from 93081812Z to 93082000Z at 12 hour intervals. The model computed directional spectra are also shown. Note that model wind speeds are larger than measured during this time period. Consequently, predicted spectra and significant wave heights also are higher than measured. The buoy wind speed and direction at 1812Z is 8.3 m/s and 200 deg (model: 10.0 m/s, 185 deg). The wind speed increases to 14.6 m/s, with the direction changes to 140 deg (model: 18.0 m/s, 147 deg) at 1900Z. The wind speed then decreases to 9.9 m/s with the direction turns slightly to 150 deg (model: 13.1 m/s, 162 deg) at 1912Z and finally, 4.1 m/s wind speed and 170 deg wind direction (model: 6.1 m/s, 158 deg) at 2000Z. In general, predicted frequencies at the spectral peaks are consistent with measured values. During growth stage, the high frequency part of the spectrum also agrees with measurement. However, the rate of wave energy

decay tends to be too slow as the wind speed decreases.

Figures 8(a) and 8(b) show examples of spectra consisting wind waves and swell simultaneously. The positions of two peaks in each model spectrum agree reasonably well with what have been measured, though somewhat over-predicting the amount of swell energy. It is interesting to see that the directional spectra predicted by the wave model have clearly distinguished dirctional orientation of wind waves which were caused by local wind from the persistent northward swell.

Wave Patterns

An inter-comparison of wave fields over the Gulf between model forecasts and hand-analyses has been made. The hand-analyses are made by marine forecasters independently based on analyzed surface weather charts, reports of wind and wave observations from ships, and measurements from moored and drifting buoys, as well as coastal marine stations (CMAN). Examples are given below for the case of the passage of a strong low pressure system across the Gulf. Figures 9(a) and 9(b) show the surface weather charts covering the Gulf area at 93081900Z and 93082000Z, respectively. Figure 10(a) shows the results of marine forecaster's analysis and model forecast at 93081900Z, while, Figure 10(b) for 93082000Z. It is interesting to observe that both analyses and forecasts have quite similar wave patterns over the Gulf. It indicating the adequacy of the Gulf of Alaska regional model in providing forecast guidance.

5. CONCLUDING REMARKS

The performance of NMC Gulf of Alaska regional wave forecast model recently implemented has been evaluated against buoy measurements for the months from April 1993 to September 1993. For up to 48 h forecasts, the mean bias of the significant wave height is 0.26 m, the root-mean-square error, 0.65 m, the correlation coefficient, 0.85, and the scatter index is 0.3. In view of various factors affecting the accuracy of wave model forecasts, the results are considered to be acceptable.

The major factor that affects the accuracy of wave forecasts is input winds. The global atmospheric model which supplies the required wind input for the wave model can not adequately take into account the complex orographic effects. Another factor that might contribute to the problem is the deficiency of the boundary wave condition provided by the global wave model.

The evaluation of model performance made in this report is by no means conclusive. Further improvement of the model is possible. The following tasks are being undertaken towards achieving this goal:

1. Collect more data to reduce sampling variability and provide more definite results in statistical sense. The results may also be used to tune the wave model.

2. Test wind products from regional atmospheric models, such as the Eta model (Black et al., 1993) for possible improvement of the wind input to the wave model.

3. Assimilate wave data obtained from ERS-1 altimeter, buoys, ships, and other surface marine observations into the wave model during the hindcasting stage.

4. Improve the global wave model forecasts for better boundary wave conditions.

6. REFERENCES

Black, T., D.Deaven and G.DiMego (1993): The step-mountain eta coordinate model: 80 km 'early' version and objective verifications. National Weather Service, Tech. Proc. Bulletin, 412, 31 pp. NOAA, Dept. of Commerce.

Collins, J.I. (1972): Prediction of shallow-water spectra, J. Geophys. Res. 77,2693-2707.

Duffy, D.G. and R. Atlas (1984): Surface wind and wave height prediction for the QEII storm using SEASAT scatterometer data. Proc. of Oceans, September 10-12,1984. refraction coefficients for sea waves. J. Geophys. Res. 65(2), 637-642.

Goldin, B.(1983): A wave prediction system for real-time sea state forecasting. Quart. J. Royal Meteor. Soc.,109,393-416.

Hasselmann, K., (1974): On the spectral dissipation of ocean waves due to white-capping, Bound.-Layer Meteor., 6(1-2) 107-127.

Hasselmann, K., et al.(1973): Measurements of wind-wave growth and swell decay during the joint North Sea wave project (JONSWAP). Ergänzungsh. Dtsch. Hydrogr. Z.,Reich A 12-95.

Hasselmann, K., Ross, D.B., Müller, P., Sell, W. (1976): A parametric wave prediction model. J. Phys. Oceanogr. 6, 200-228.

Kanamitsu, M., J.C. Alpert, K. A., Campana, P. M. Caplan, D.G. Deaven, M. Iredell, B. Katz, H.L.Pan, J.E. Sela and G.H. White (1991): Recent changes implemented into the global forecast system at NMC. Wea. Forecasting, 6, 425-435.

Parrish, D.F. and J.C. Derber(1992): The National Meteorological Center's spectral statistical-interpolation analysis system. Mon. Wea. Rev., 120, 1747-1763.

Pierson, W.J. and L. Moskowitz(1964): A proposed spectral form of fully developed wind seas based on the similarity theory of S.A. Kitaigorodskii. J. Geophys. Res., 69(24),5181-5190.

Shemdin, O.H., S.V. Hsiao, H.E. Carlson, K. Hasselmann, and K. Schulze (1980): Mechanisms of wave transformation in finite-depth water. J. Geophys. Res. 85(C9) 5012-5018.

Sleath, J.F.H.(1970): Wave-induced pressures in beds of sand. J. Hydrol. Div., HY2, 367-378.

Snyder, R.L., F.W. Dobson, J.A. Elliot and R.B. Long (1981): Array measurements of atmospheric pressure fluctuations above surface gravity waves, J. Fluid Mech., 102,1-59.

Steele, K.E., J.C.K. Lau, and Y.-H.L. Hsu (1985): Theory and application of calibration techniques for an NDBC directional wave measurements buoy. IEEE J. Oceanic Engng. OE-10, 382-396.

Steele, K.E., C.-C. Teng and D.W.C. Wang (1992): Wave direction measurements using pitch-roll buoys. Ocean Engng., 4, 349-375.

SWAMP Group (1985): Ocean Wave Modeling. Plenum Press, New York, 256 pp.

Takacs, L.(1985): A two-step scheme for the advection equation with minimum dissipation and dispersion errors. Mon. Wea. Rev., 113, 1050-1065.

Thornton, E.B.(1977): Redrivation of the saturation range in the frequency spectrum of wind-generated gravity waves. J. Phys. Oceano., 7, 137.

FIGURE CAPTIONS

Figure 1 Area of interest.

Figure 2 General flow of numerical models involved in wind and wave forecasts, including starting times of runs and forecast lengths.

Figure 3 Scatter diagrams of the initial wave and wind conditions of the GAK model and buoy measurements at Buoy 46001.

Figure 4 Scatter diagrams of GAK model forecast and buoy measured significant wave heights at Buoy 46001 for four projection hours.

Figure 5(a) Scatter diagrams of model forecast and buoy measured wind speeds at Buoy 46001 for four projection hours.
Figure 5(b) Scatter diagrams of the model forecast and buoy measured wind directions at Buoy 46001 for four projection hours.

Figure 6 Scatter diagrams of NOW model forecast and buoy measured significant wave heights at Buoy 46001 for four projection hours.

Figure 7(a) Comparisons of GAK model forecast and buoy measured wave spectra during the stage of wave growth.
Figure 7(b) Comparisons of GAK model forecast and buoy measured wave spectra during the stage of wave decay.

Figure 8(a) Comparisons of GAK model forecast and buoy measured wave spectra at 93091012Z and 93091100Z when sea and swell exist simultaneously.
Figure 8(b) Comparisons of GAK model forecast and buoy measured wave spectra at 93091112Z and 93091200Z when sea and swell exist simultaneously.

Figure 9 Surface weather charts for the Gulf of Alaska area during the passage of a low pressure system.
(a) August 19, 0000Z, 1993
(b) August 20, 0000Z, 1993

Figure 10(a) Comparison of model forecat and independent hand-analysis of the wave height pattern over the Gulf for August 19, 0000Z, 1993.
Figure 10(b) Comparison of model forecat and independent hand-analysis of the wave height pattern over the Gulf for August 20, 0000Z, 1993.

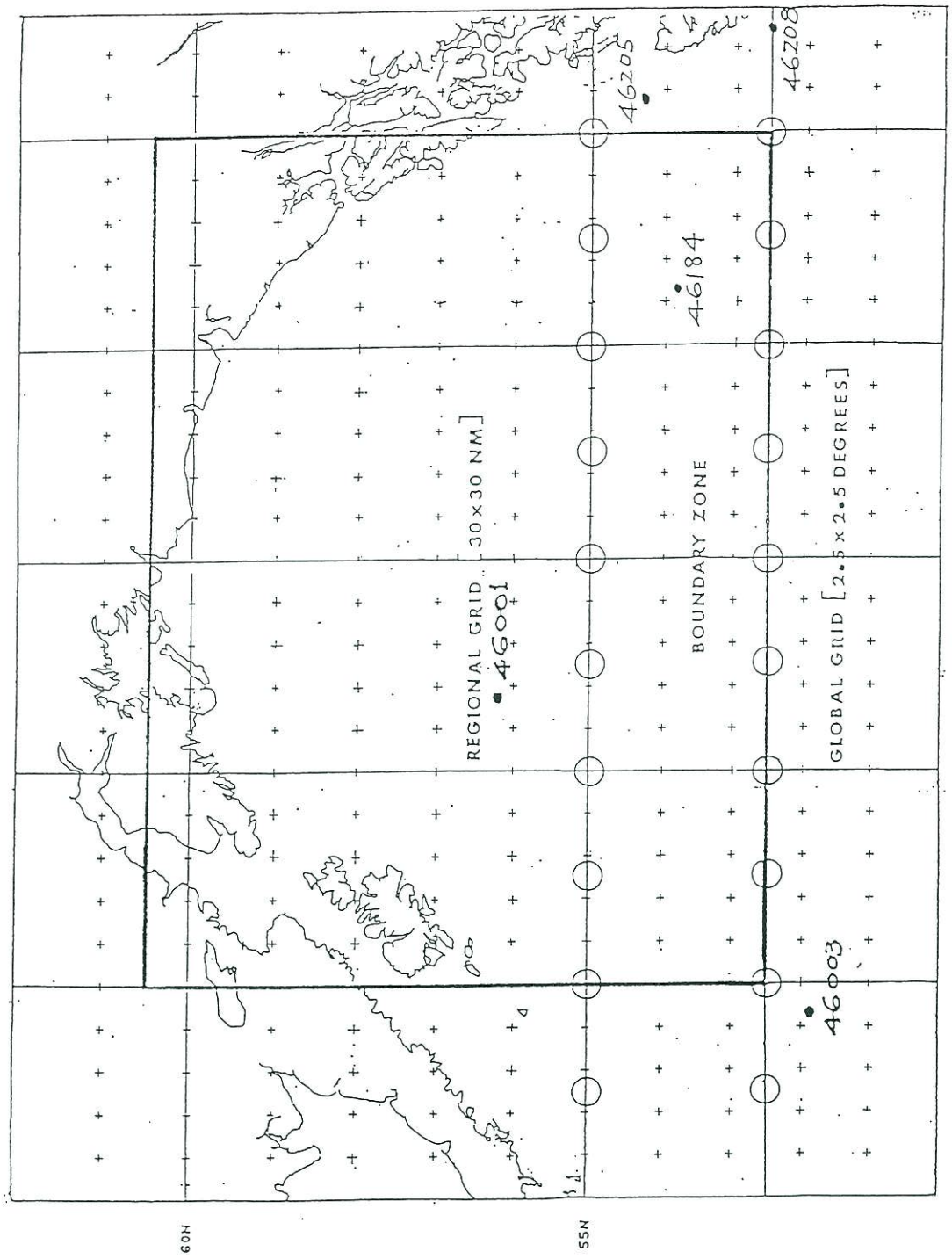

Figure 1. Area of interest.

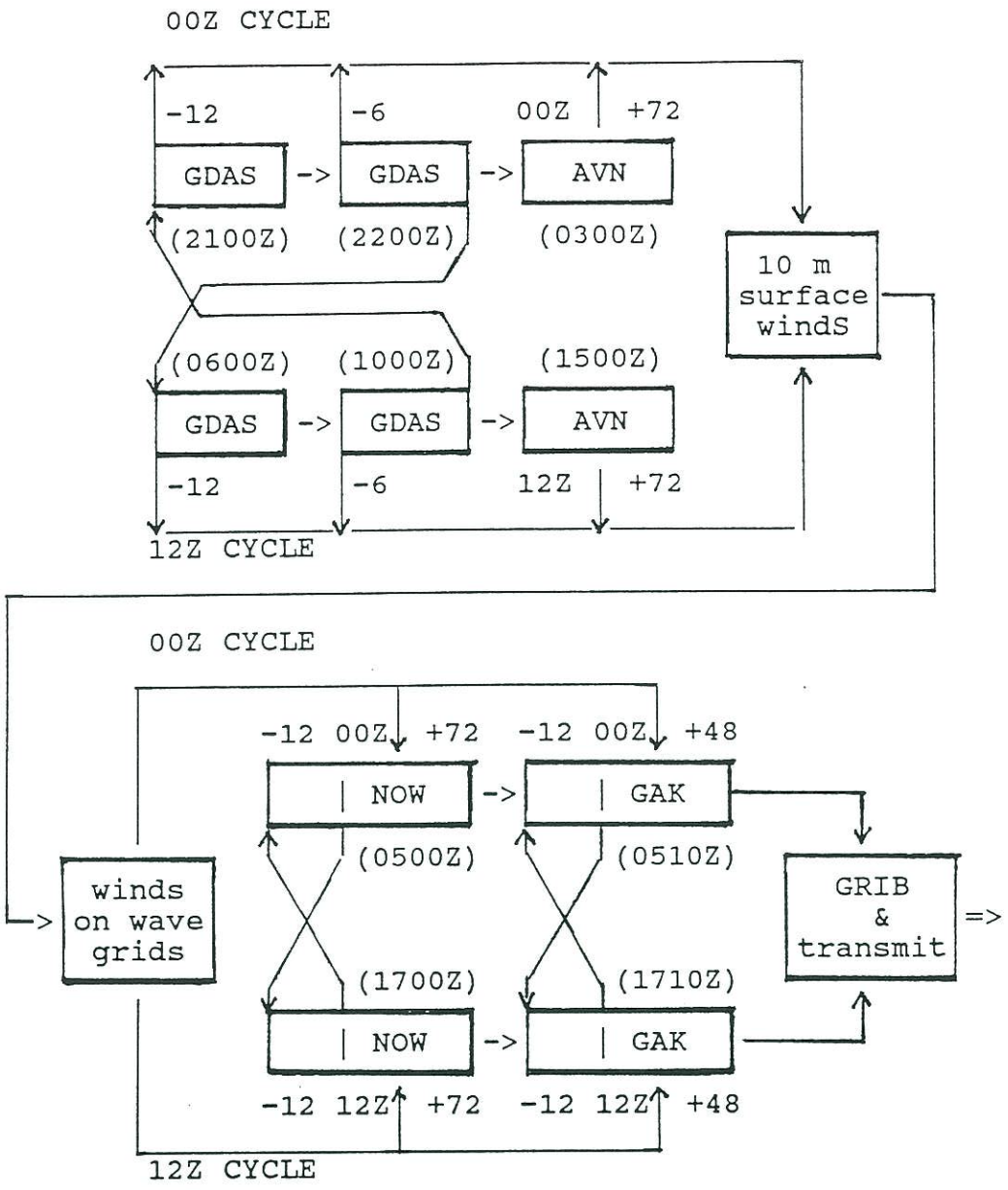

AFOS: Automation of Field Operation and Services
AVN: AViatioN run of global atmospheric model
GAK: Gulf of AlasKa wave model
GDAS: Global Data Assimilation System
NOW: NOAA global Ocean Wave model
GRIB: wave model output in GRIdded Binary form
(....Z): scheduled starting time for computation

Figure 2. General flow of numerical models involved in wind and wave forecasts, including starting times of runs and forecast lengths.

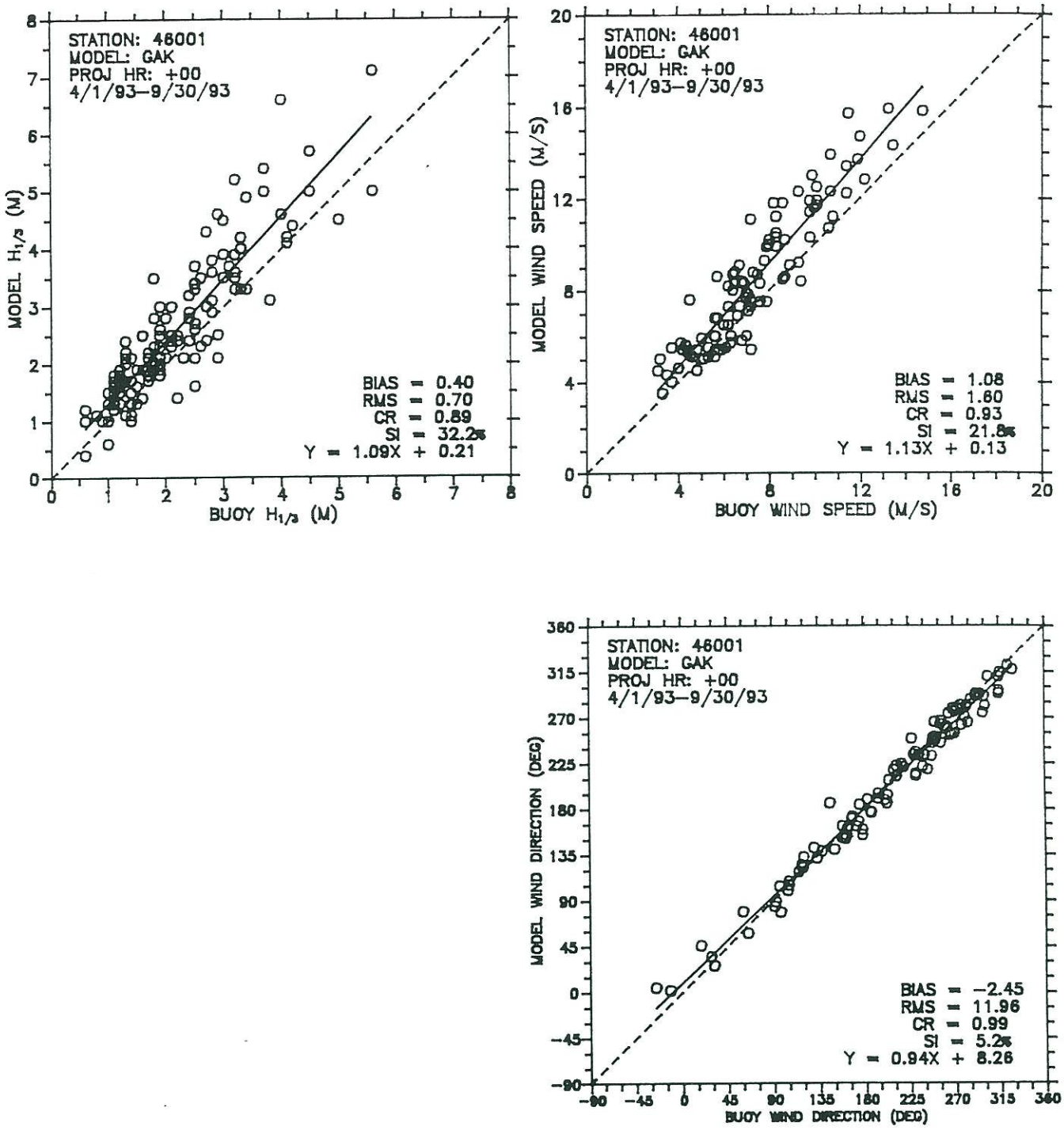

Figure 3. Scatter diagrams of the initial wave and wind conditions of the GAK model and buoy measurements at Buoy 46001.

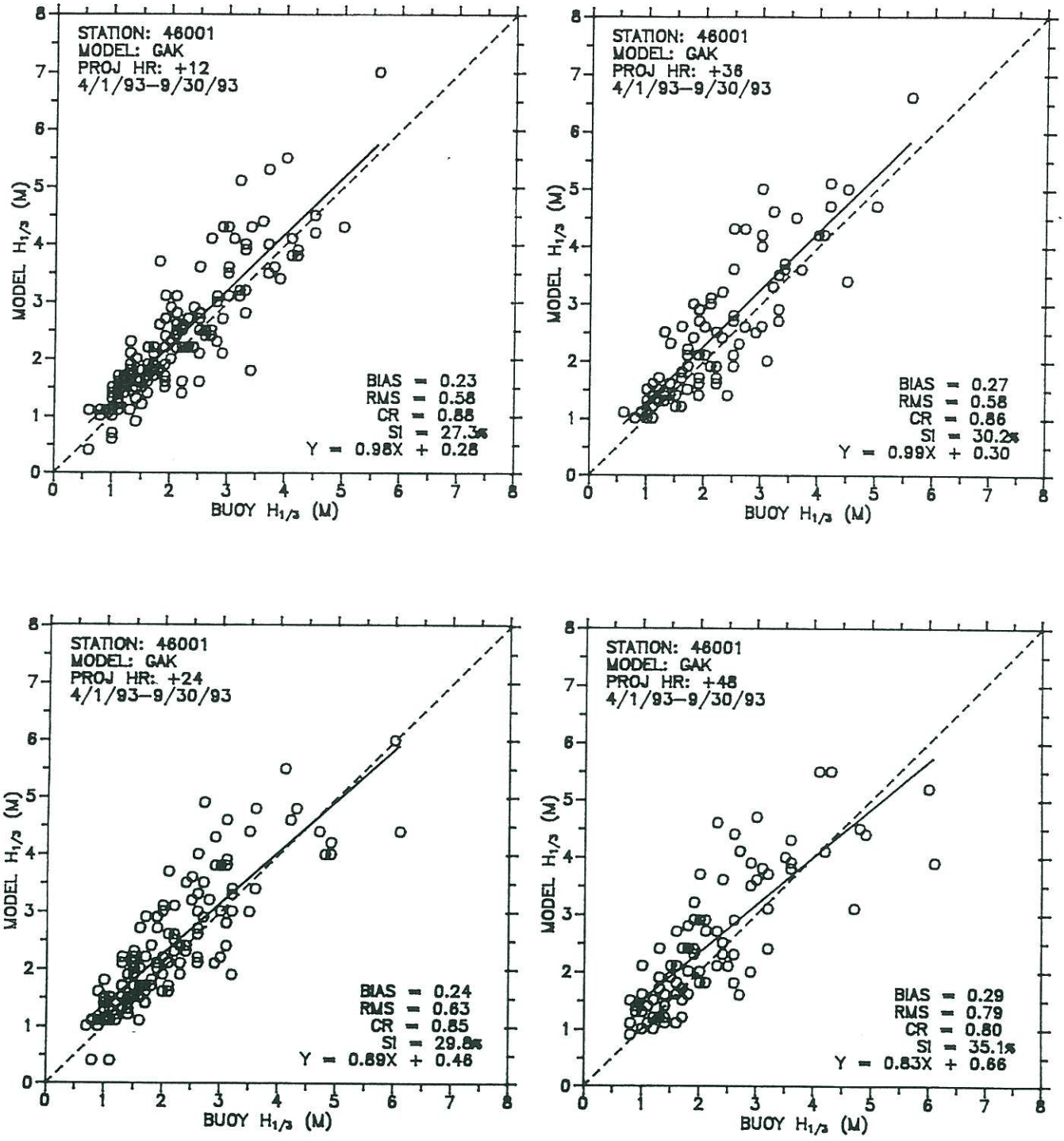

Figure 4. Scatter diagrams of GAK model forecast and buoy measured significant wave heights at Buoy 46001 for four projection hours.

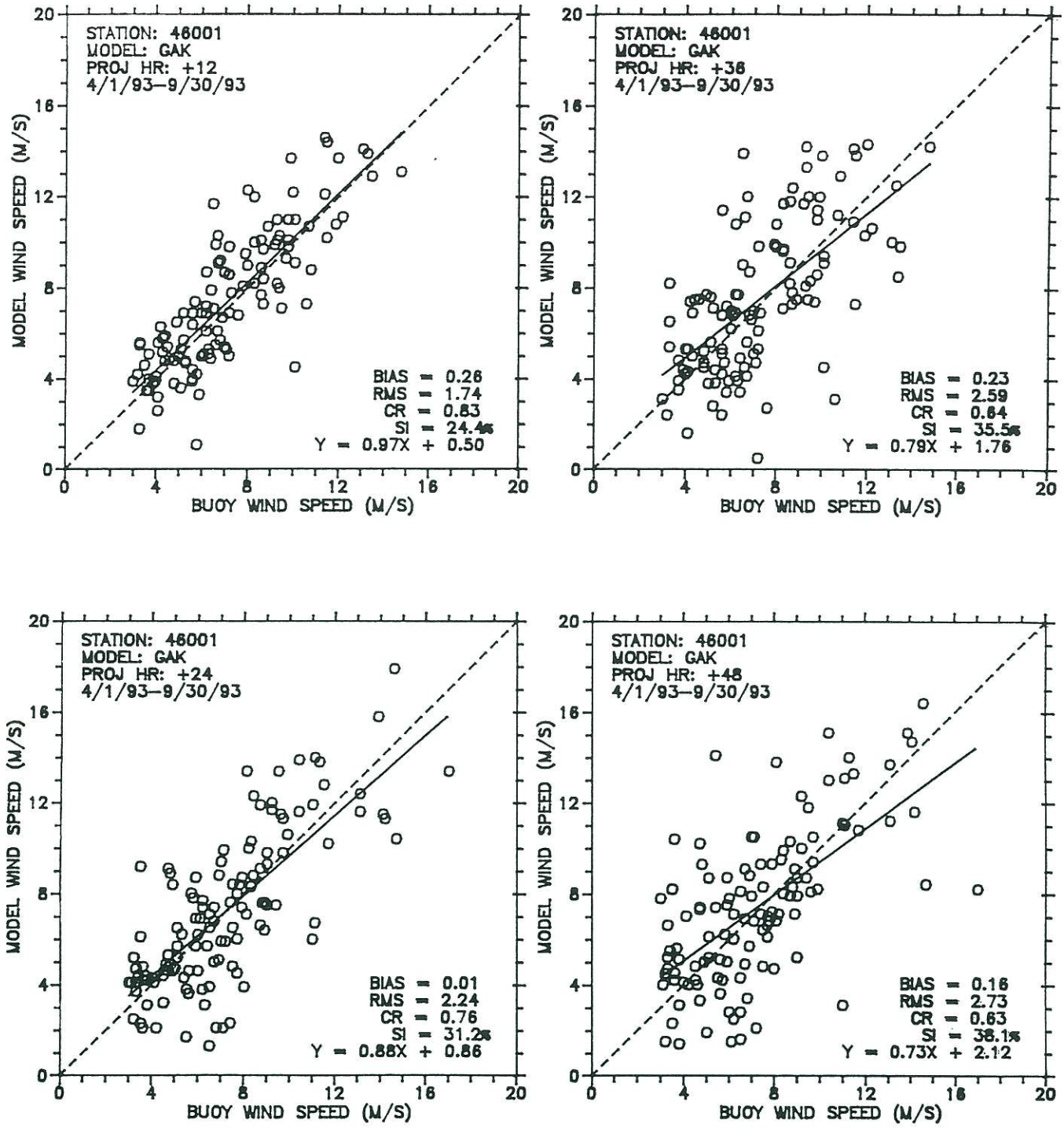

Figure 5(a). Scatter diagrams of model forecast and buoy measured wind speeds at Buoy 46001 for four projection hours.

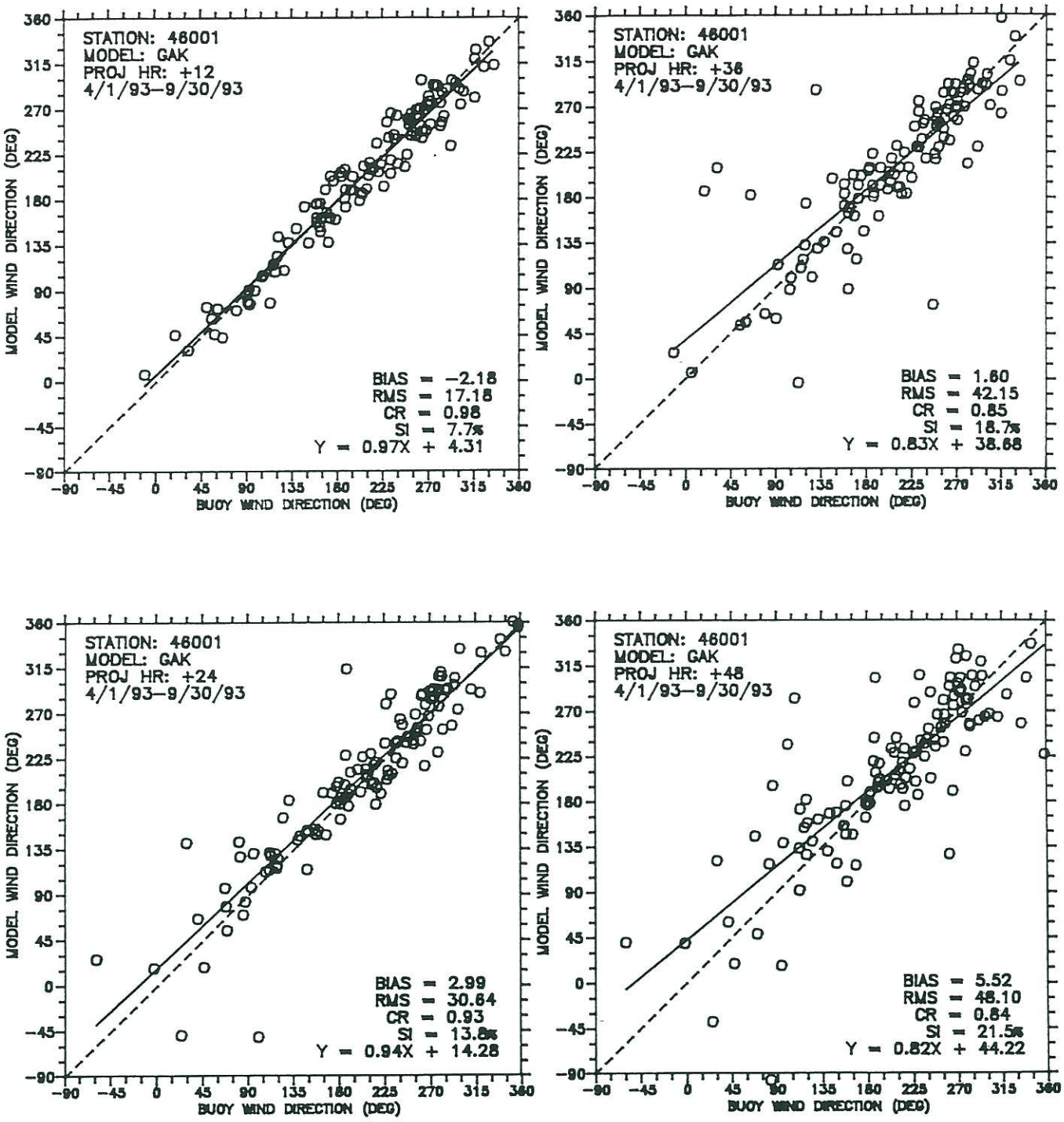

Figure 5(b). Scatter diagrams of the model forecast and buoy measured wind directions at Buoy 46001 for four projection hours.

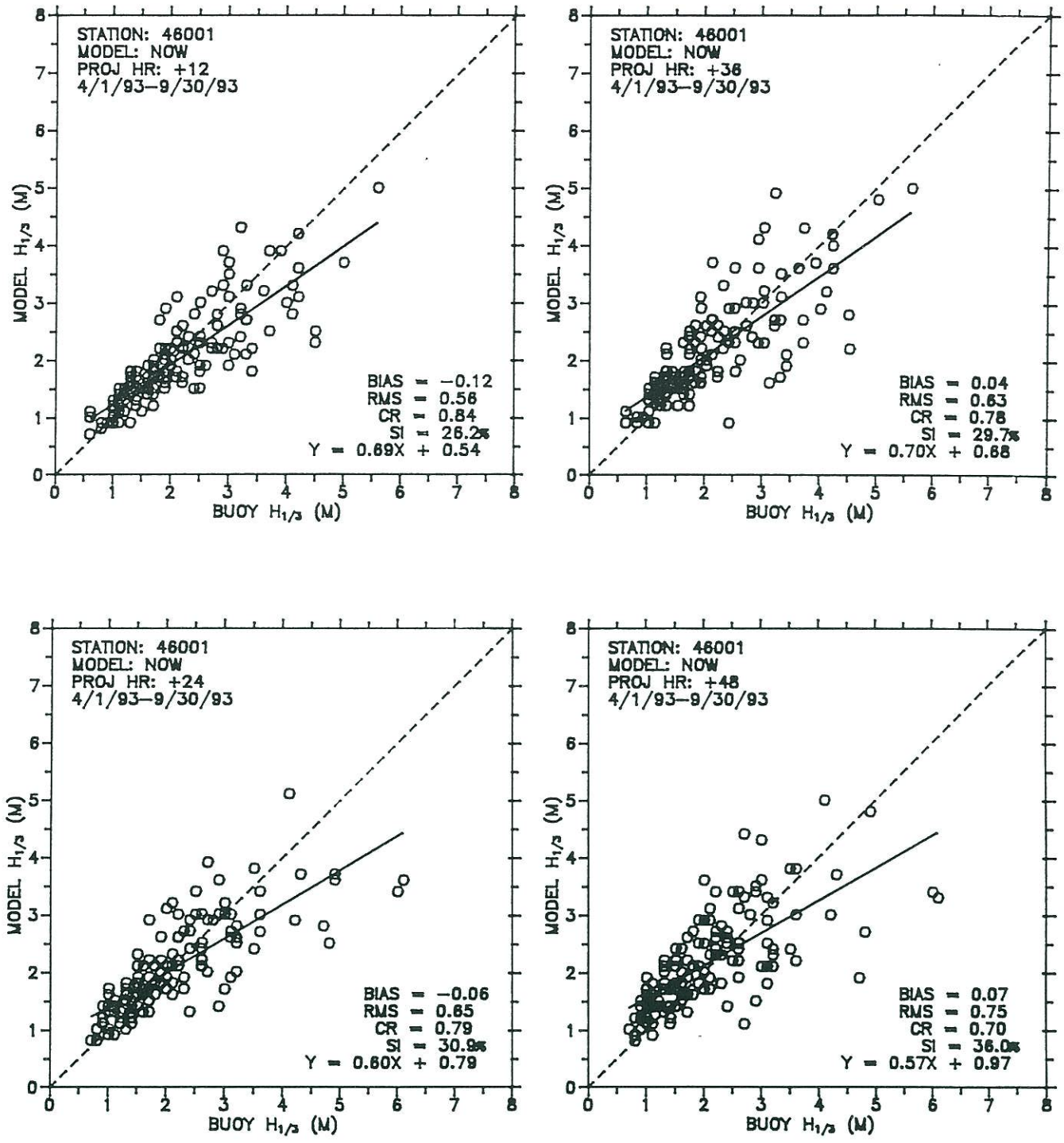

Figure 6. Scatter diagrams of NOW model forecast and buoy measured significant wave heights at Buoy 46001 for four projection hours.

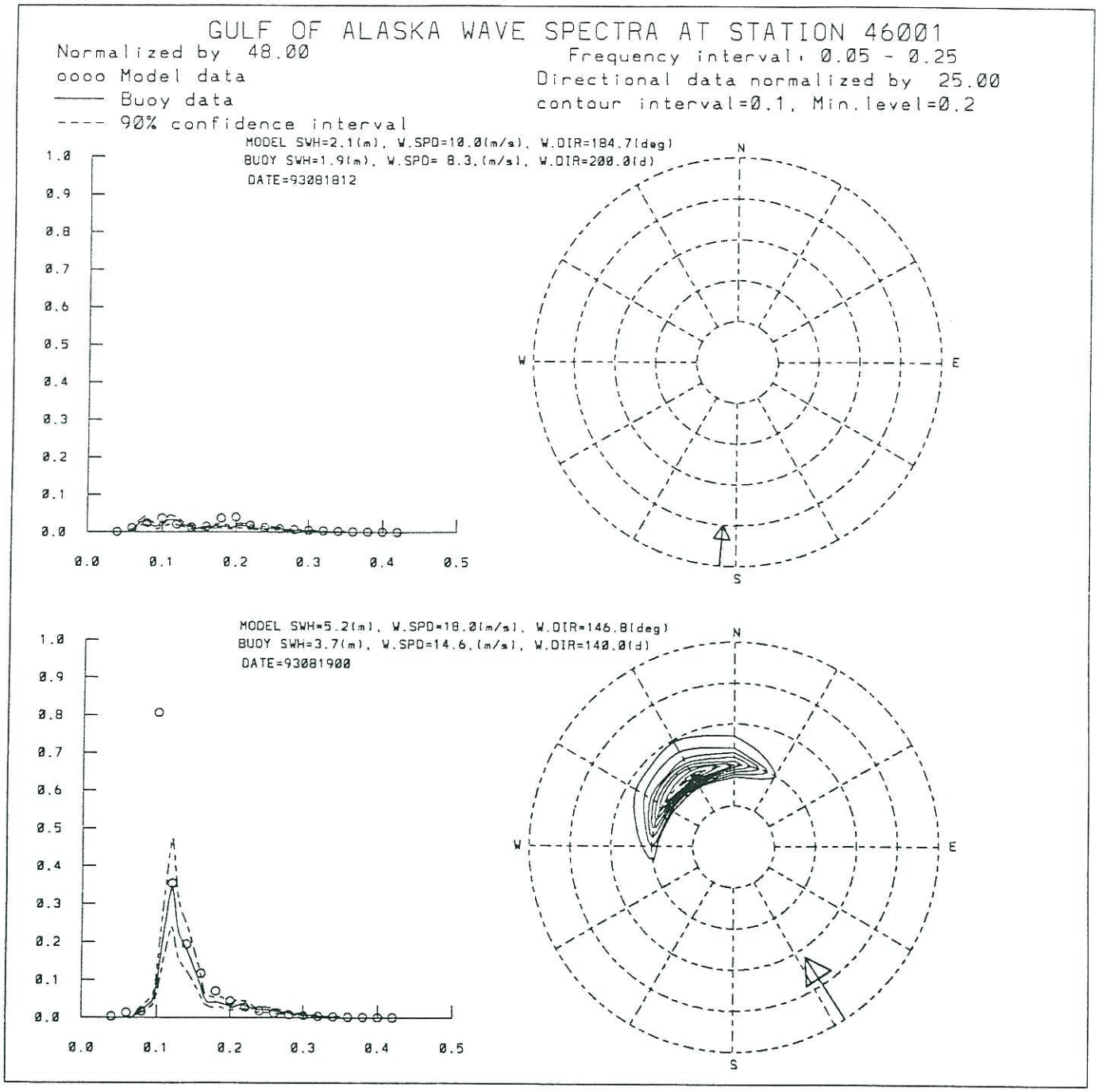

Figure 7(a). Comparisons of GAK model forecast and buoy measured wave spectra during the stage of wave growth.

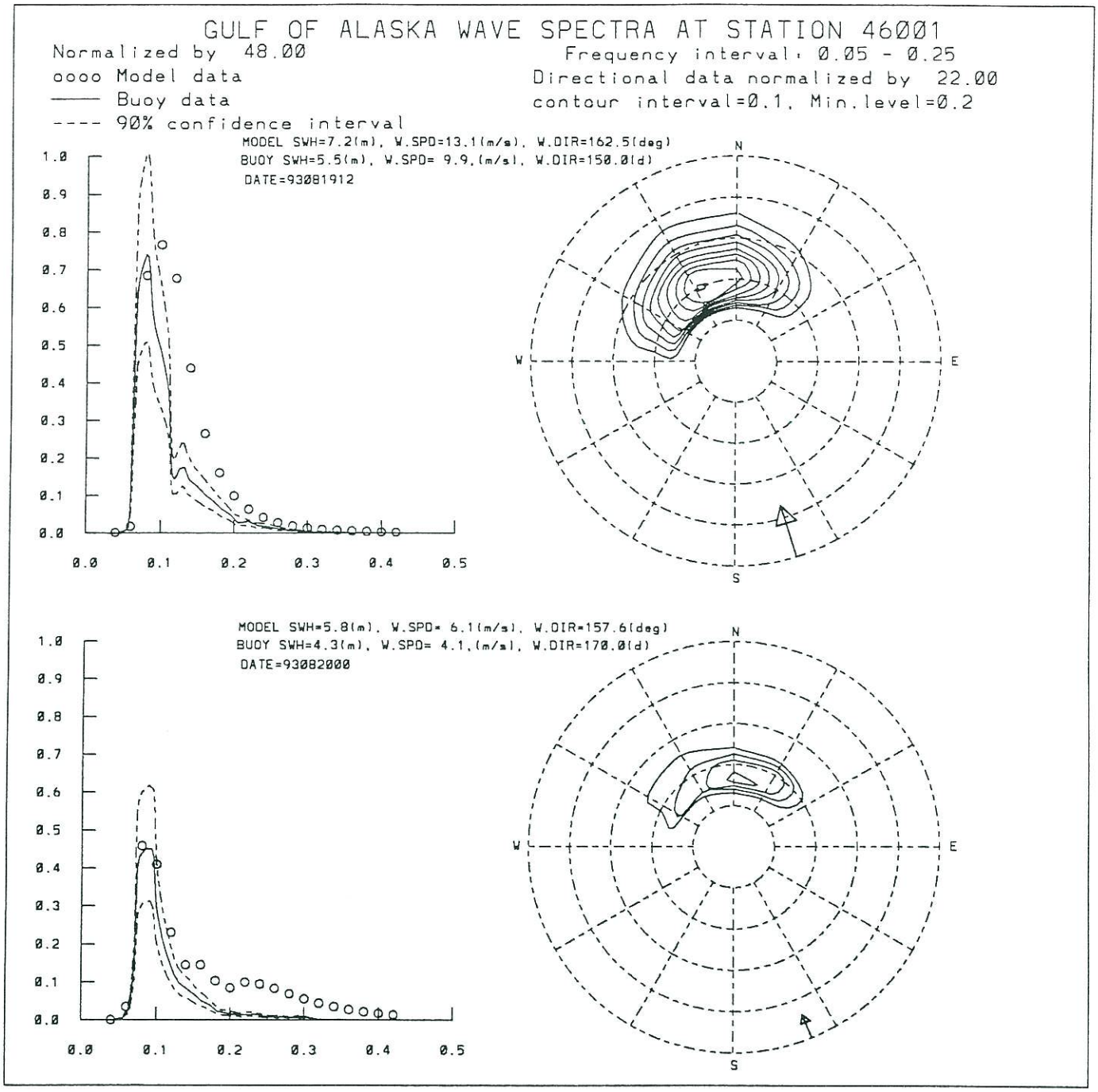

Figure 7(b). Comparisons of GAK model forecast and buoy measured wave spectra during the stage of wave decay.

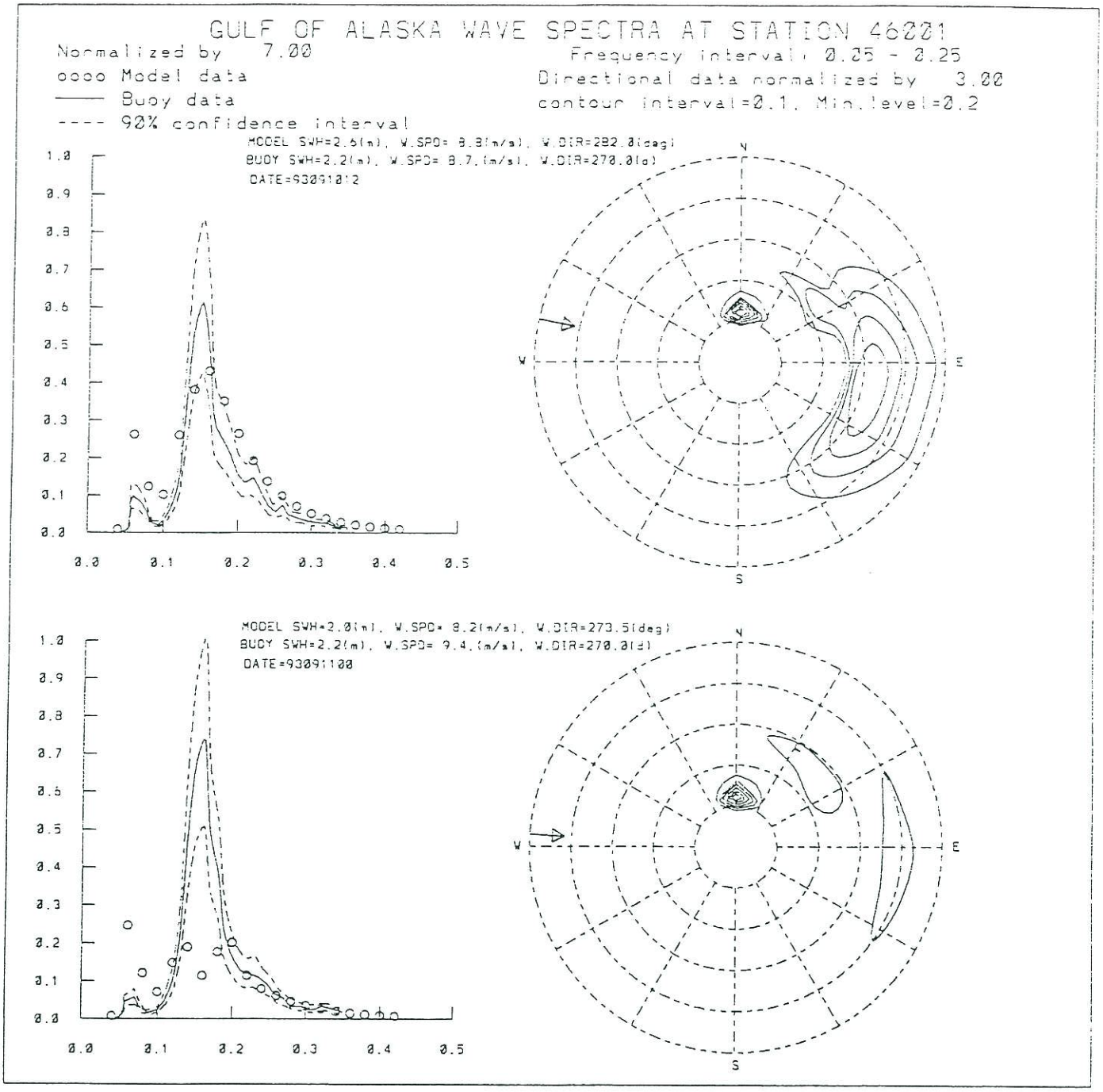

Figure 8(a). Comparisons of GAK model forecast and buoy measured wave spectra at 93091012Z and 93091100Z when sea and swell exist simultaneously.

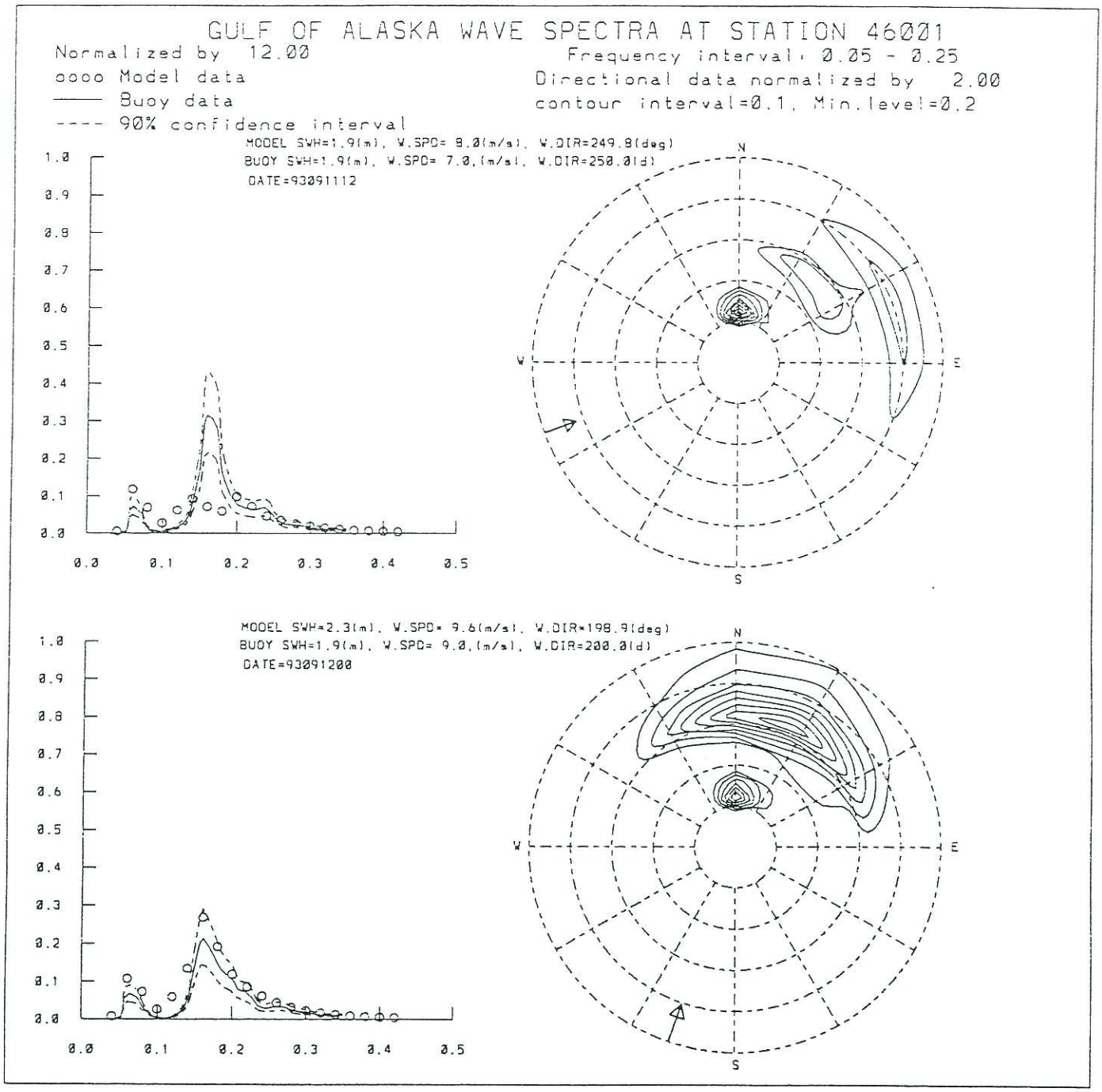

Figure 8(b). Comparisons of GAK model forecast and buoy measured wave spectra at 93091112Z and 93091200Z when sea and swell exist simultaneously.

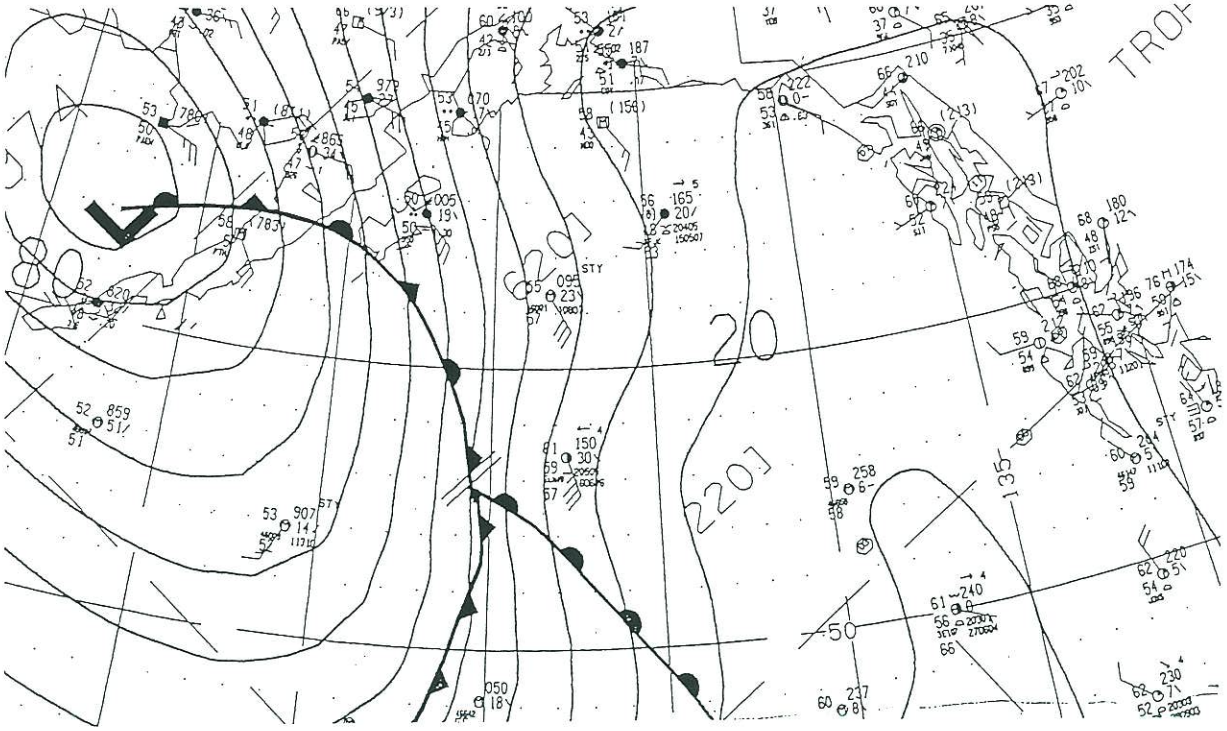

(a)

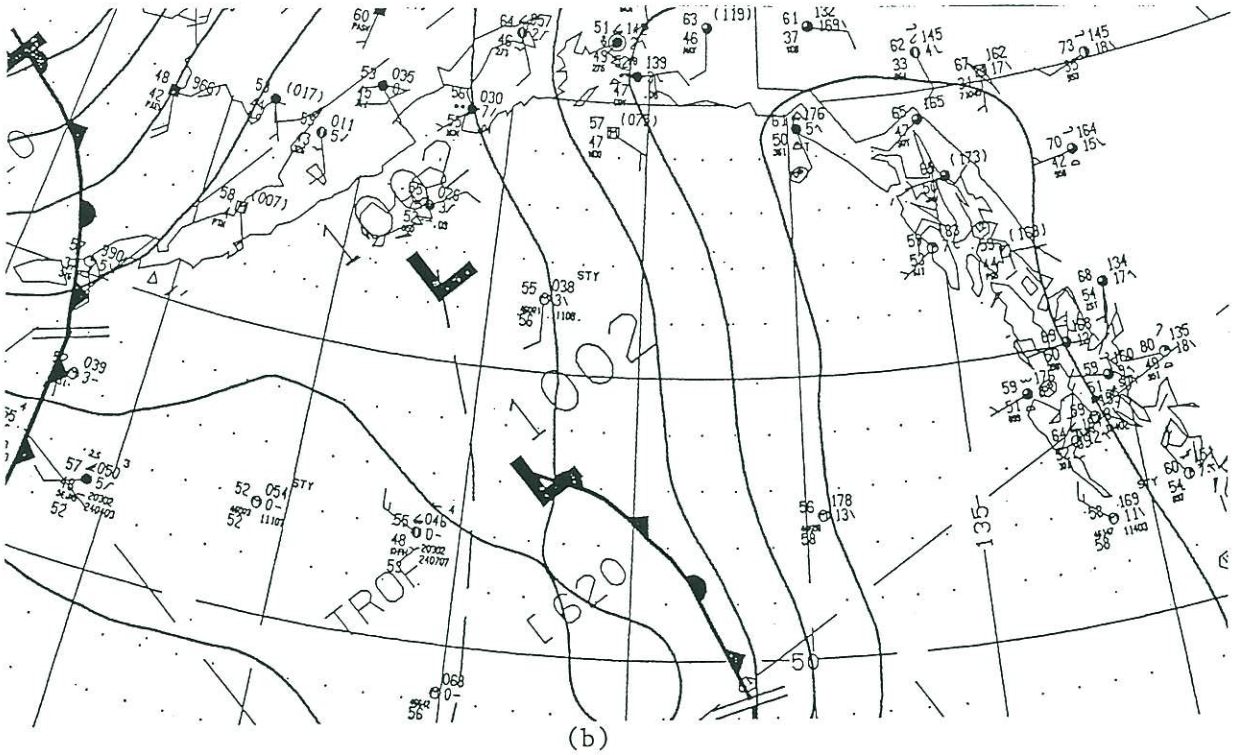

(b)

Figure 9. Surface weather charts for the Gulf of Alaska area during the passage of a low pressure system.
(a). August 19, 0000Z, 1993
(b). August 20, 0000Z, 1993

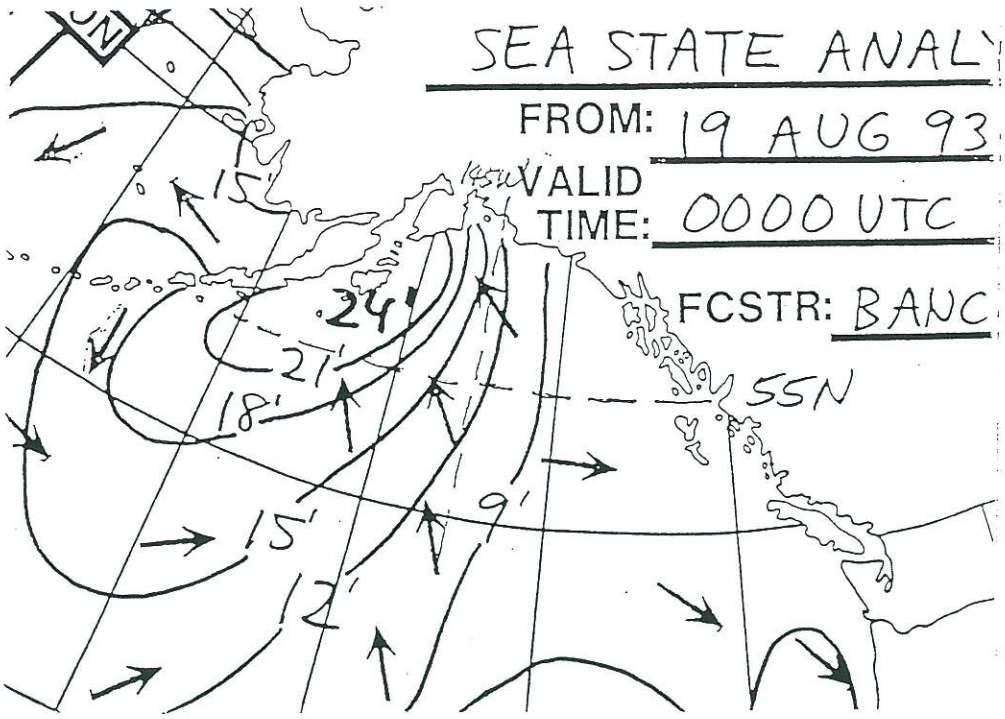

GULF OF ALASKA, FCST HR&VALID DATE = 24 93081900
Significant Wave Height(ft), Wind Speed & Direction
PARALLEL RUN

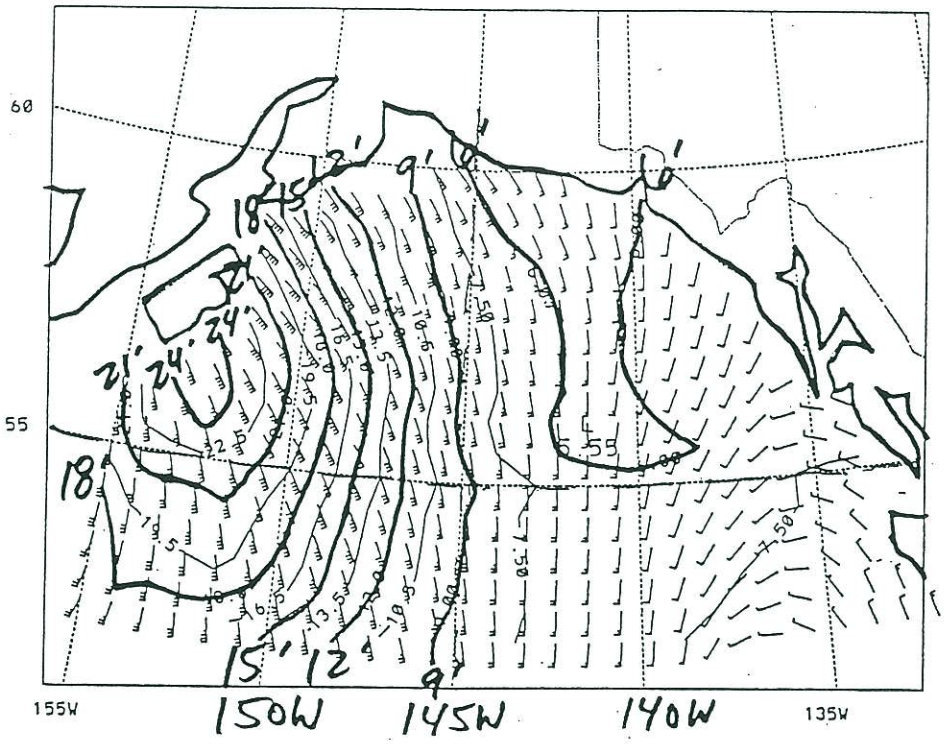

Figure 10(a). Comparison of model forecast and independent hand-analysis of the wave height pattern over the Gulf for August 19, 0000Z, 1993.

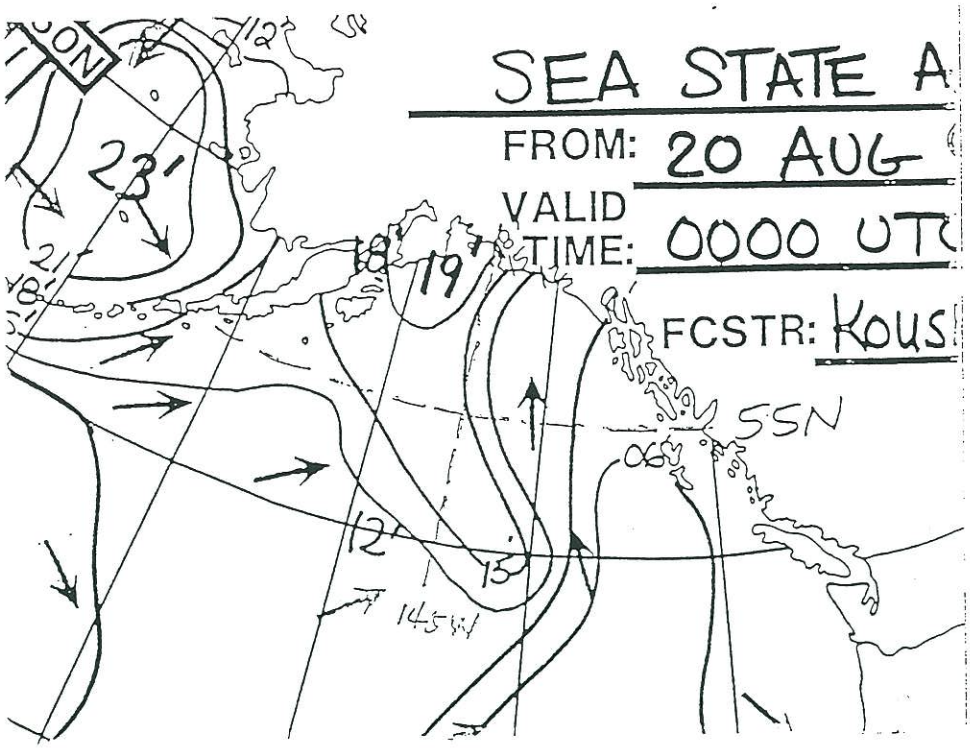

GULF OF ALASKA. FCST HR&VALID DATE = 24 93087000
Significant Wave Height(ft), Wind Speed & Direction
PARALLEL RUN

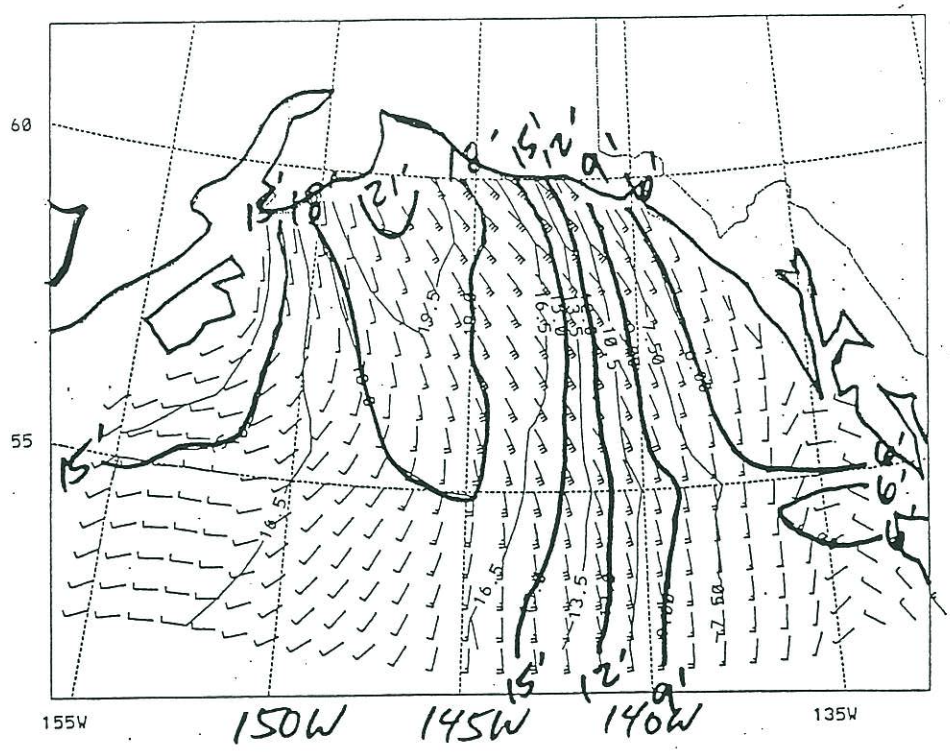

Figure 10(b.). Comparison of model forecast and independent hand-analysis of the wave height pattern over the Gulf for August 20, 0000Z, 1993.

No. 19. Esteva, D.C., 1988: Evaluation of Priliminary Experiments Assimilating Seasat Significant Wave Height into a Spectral Wave Model. Journal of Geophysical Research. 93, 14,099-14,105

No. 20. Chao, Y.Y., 1988: Evaluation of Wave Forecast for the Gulf of Mexico. Proceedings Fourth Conference Meteorology and Oceanography of the Coastal Zone, 42-49

No. 21. Breaker, L.C., 1989: El Nino and Related Variability in Sea-Surface Temperature Along the Central California Coast. PACLIM Monograph of Climate Variability of the Eastern North Pacific and Western North America, Geophysical Monograph 55, AGU, 133-140.

No. 22. Yu, T.W., D.C. Esteva, and R.L. Teboulle, 1991: A Feasibility Study on Operational Use of Geosat Wind and Wave Data at the National Meteorological Center. Technical Note/NMC Office Note No. 380, 28pp.

No. 23. Burroughs, L. D., 1989: Open Ocean Fog and Visibility Forecasting Guidance System. Technical Note/NMC Office Note No. 348, 18pp.

No. 24. Gerald, V. M., 1987: Synoptic Surface Marine Data Monitoring. Technical Note/NMC Office Note No. 335, 10pp.

No. 25. Breaker, L. C., 1989: Estimating and Removing Sensor Induced Correlation form AVHRR Data. Journal of Geophysical Reseach, 95, 9701-9711.

No. 26. Chen, H. S., 1990: Infinite Elements for Water Wave Radiation and Scattering. International Journal for Numerical Methods in Fluids, 11, 555-569.

No. 27. Gemmill, W.H., T.W. Yu, and D.M. Feit, 1988: A Statistical Comparison of Methods for Determining Ocean Surface Winds. Journal of Weather and Forecasting. 3, 153-160.

No. 28. Rao. D. B., 1989: A Review of the Program of the Ocean Products Center. Weather and Forecasting. 4, 427-443.

No. 29. Chen, H. S., 1989: Infinite Elements for Combined Diffration and Refraction . Conference Preprint, Seventh International Conference on Finite Element Methods Flow Problems, Huntsville, Alabama, 6pp.

NO. 30. Chao, Y. Y., 1989: An Operational Spectral Wave Forecasting Model for the Gulf of Mexico. Proceedings of 2nd International Workshop on Wave Forecasting and Hindcasting, 240-247.

No. 31. Esteva, D. C., 1989: Improving Global Wave Forecasting Incorporating Altimeter Data. Proceedings of 2nd International Workshop on Wave Hindcasting and Forecasting, Vancouver, B.C., April 25-28, 1989, 378-384.

No. 32. Richardson, W. S., J. M. Nault, D. M. Feit, 1989: Computer-Worded Marine Forecasts. Preprint, 6th Symp. on Coastal Ocean Management Coastal Zone 89, 4075-4084.

No. 33. Chao, Y. Y., T. L. Bertucci, 1989: A Columbia River Entrance Wave Forecasting Program Developed at the Ocean Products Center. Techical Note/NMC Office Note 361.

No. 34. Burroughs, L. D., 1989: Forecasting Open Ocean Fog and Visibility. Preprint, 11th Conference on Probability and Statisitcs, Monterey, Ca., 5pp.

No. 35. Rao, D. B., 1990: Local and Regional Scale Wave Models. Proceeding (CMM/WMO) Technical Conference on Waves, WMO, Marine Meteorological of Related Oceanographic Activities Report No. 12, 125-138.

No. 36. Burroughs, L.D., 1991: Forecast Guidance for Santa Ana conditions. Technical Procedures Bulletin No. 391, 11pp.

No. 37. Burroughs, L. D., 1989: Ocean Products Center Products Review Summary. Technical Note/NMC Office Note No. 359. 29pp.

No. 38. Feit, D. M., 1989: Compendium of Marine Meteorological and Oceanographic Products of the Ocean Products Center (revision 1). NOAA Technical Memo NWS/NMC 68.

No. 39. Esteva, D. C., Y. Y. Chao, 1991: The NOAA Ocean Wave Model Hindcast for LEWEX. Directional Ocean Wave Spectra, Johns Hopkins University Press, 163-166.

No. 40. Sanchez, B. V., D. B. Rao, S. D. Steenrod, 1987: Tidal Estimation in the Atlantic and Indian Oceans, 3° x 3° Solution. NASA Technical Memorandum 87812, 18pp.

No. 41. Crosby, D.S., L.C. Breaker, and W.H. Gemmill, 1990: A Difintion for Vector Correlation and its Application to Marine Surface Winds. Technical Note/NMC Office Note No. 365, 52pp.

No. 42. Feit, D.M., and W.S. Richardson, 1990: Expert System for Quality Control and Marine Forecasting Guidance. Preprint, 3rd Workshop Operational and Metoerological. CMOS, 6pp.

No. 43. Gerald, V.M., 1990: OPC Unified Marine Database Verification System. Technical Note/NMC Office Note No. 368, 14pp.

No. 44. Wohl, G.M., 1990: Sea Ice Edge Forecast Verification System. National Weather Association Digest, (submitted)

No. 45. Feit, D.M., and J.A. Alpert, 1990: An Operational Marine Fog Prediction Model. NMC Office Note No. 371, 18pp.

No. 46. Yu, T. W. , and R. L. Teboulle, 1991: Recent Assimilation and Forecast Experiments at the National Meteorological Center Using SEASAT-A Scatterometer Winds. Technical Note/NMC Office Note No. 383, 45pp.

No. 47. Chao, Y.Y., 1990: On the Specification of Wind Speed Near the Sea Surface. Marine Forecaster Training Manual, (submitted)

No. 48. Breaker, L.C., L.D. Burroughs, T.B. Stanley, and W.B. Campbell, 1992: Estimating Surface Currents in the Slope Water Region Between 37 and 41°N Using Satellite Feature Tracking. Technical Note, 47pp.

No. 49. Chao, Y.Y., 1990: The Gulf of Mexico Spectral Wave Forecast Model and Products. Technical Procedures Bulletin No. 381, 3pp.

No. 50. Chen, H.S., 1990: Wave Calculation Using WAM Model and NMC Wind. Preprint, 8th ASCE Engineering Mechanical Conference, 1, 368-372.

No. 51. Chao, Y.Y., 1990: On the Transformation of Wave Spectra by Current and Bathymetry. Preprint, 8th ASCE Engineering Mechnical Conference, 1, 333-337.

No. 52. Breaker, L.C., W.H. Gemmill, and D.S. Crosby, 1990: A Vector Correlation Coefficient in Geophysical: Theoretical Background and Application. Deep Sea Research, (to be submitted)

No. 53. Rao, D.B., 1991: Dynamical and Statistical Prediction of Marine Guidance Products. Proceedings, IEEE Conference Oceans 91, 3, 1177-1180.

No. 54. Gemmill, W.H., 1991: High-Resolution Regional Ocean Surface Wind Fields. Proceedings, AMS 9th Conference on Numerical Weather Prediction, Denver, CO, Oct. 14-18, 1991, 190-191.

No. 55. Yu, T.W., and D. Deaven, 1991: Use of SSM/I Wind Speed Data in NMC's GDAS. Proceedings, AMS 9th Conference on Numerical Weather Prediction, Denver, CO, Oct. 14-18, 1991, 416-417.

No. 56. Burroughs, L.D., and J.A. Alpert, 1992: Numerical Fog and Visiability Guidance in Coastal Regions. Technical Procedures Bulletin. (to be submitted)

No. 57. Chen, H.S., 1992: Taylor-Gelerkin Method for Wind Wave Propagation. ASCE 9th Conf. Eng. Mech. (in press)

No. 58. Breaker, L.C., and W.H. Gemmill, and D.S. Crosby, 1992: A Technique for Vector Correlation and its Application to Marine Surface Winds. AMS 12th Conference on Probability and Statistics in the Atmospheric Sciences, Toronto, Ontario, Canada, June 22-26, 1992.

No. 59. Breaker, L.C., and X.-H. Yan, 1992: Surface Circulation Estimation Using Image Processing and Computer Vision Methods Applied to Sequential Satellite Imagery. Proceeding of the 1st Thematic Conference on Remote Sensing for Marine Coastal Environment, New Orleans, LA, June 15-17, 1992.

No. 60. Wohl, G., 1992: Operational Demonstration of ERS-1 SAR Imagery at the Joint Ice Center. Proceeding of the MTS 92 - Global Ocean Partnership, Washington, DC, Oct. 19-21, 1992.

No. 61. Waters, M.P., Caruso, W.H. Gemmill, W.S. Richardson, and W.G. Pichel, 1992: An Interactive Information and Processing System for the Real-Time Quality Control of Marine Meteorological Oceanographic Data. Pre-print 9th International Conference on Interactive Information and Processing System for Meteorology, Oceanography and Hydrology, Anaheim, CA, Jan 17-22, 1993.

No. 62. Breaker, L.C., and V. Krasnopolsky, 1992: The Problem of AVHRR Image Navigation Revisited. Intr. Journal of Remote Sensing (in press).

No. 63. Breaker, L.C., D.S. Crosby, and W.H. Gemmill, 1992: The Application of a New Definition for Vector Correlation to Problems in Oceanography and Meteorology. Journal of Atmospheric and Oceanic Technology (submitted).

No. 64. Grumbine, R., 1993: The Thermodynamic Predictability of Sea Ice. Journal of Glaciology, (in press).

No. 65. Chen, H.S., 1993: Global Wave Prediction Using the WAM Model and NMC Winds. 1993 International Conference on Hydro Science and Engineering, Washington, DC, June 7 - 11, 1993. (submitted)

No. 66. Krasnopolsky, V., and L.C. Breaker, 1993: Multi-Lag Predictions for Time Series Generated by a Complex Physical System using a Neural Network Approach. Journal of Physics A: Mathematical and General, (submitted).

No. 67. Breaker, L.C., and Alan Bratkovich, 1993: Coastal-Ocean Processes and their Influence on the Oil Spilled off San Francisco by the M/V Puerto Rican. Marine Environmental Research, (submitted)

No. 68. Breaker, L.C., L.D. Burroughs, J.F. Culp, N.L. Gunasso, R. Teboulle, and C.R. Wong, 1993: Surface and Near-Surface Marine Observations During Hurricane Andrew. Technical Notes/NMC Office Note #398, 41pp.

No. 69. Burroughs, L.D., and R. Nichols, 1993: The National Marine Verification Program, Technical Note/NMC Office Note #393, 21pp.

No. 70. Gemmill, W.H., and R. Teboulle, 1993: The Operational Use of SSM/I Wind Speed Data over Oceans. Pre-print 13th Conference on Weather Analyses and Forecasting, (submitted).

No. 71. Yu, T.-W., J.C. Derber, and R.N. Hoffman, 1993: Use of ERS-1 Scatterometer Backscattered Measurements in Atmospheric Analyses. Pre-print 13th Conference on Weather Analyses and Forecasting, (submitted).

No. 72. Chalikov, D. and Y. Liberman, 1993: Director Modeling of Nonlinear Waves Dynamics. J. Physical, (submitted).

No. 73. Woiceshyn, P., T.W. Yu, W.H. Gemmill, 1993: Use of ERS-1 Scatterometer Data to Derive Ocean Surface Winds at NMC. Pre-print 13th Conference on Weather Analyses and Forecasting, (submitted).

No. 74. Grumbine, R.W., 1993: Sea Ice Prediction Physics. Technical Note/NMC Office Note #396, 44pp.

No. 75. Chalikov, D., 1993: The Parameterization of the Wave Boundary Layer. Journal of Physical Oceanography, (to be submitted).

No. 76. Tolman, H.L., 1993: Modeling Bottom Friction in Wind-Wave Models. Waves 93 in New Orleans, LA, (in press).

No. 77. Breaker, L., W. Broenkow, 1993: The Circulation of Monterey Bay and Related Processes. Revised and resubmitted to Oceanography and Marine Biology: An Annual Review, (to be submitted).

No. 78. Chalikov, D., D. Esteva, M. Iredell and P. Long, 1993: Dynamic Coupling between the NMC Global Atmosphere and Spectral Wave Models. Technical Note/NMC Office Note #395, 62pp.

No. 79. Burroughs, L.D., 1993: National Marine Verification Program - Verification Statistics. Technical Note/NMC Office Note #400, 49 pp.

No. 80. Shashy, A.R., H.G. McRandal, J. Kinnard, and W.S. Richardson, 1993: Marine Forecast Guidance from an Interactive Processing System. 74th AMS Annual Meeting, January 23 - 28, 1994.

No. 81. Chao, Y.Y., 1993: The Time Dependent Ray Method for Calculation of Wave Transformation on Water of Varying Depth and Current. Wave 93 ASCE. (submitted)

No. 82. Tolman, H.L., 1994: Wind-Waves and Moveable-Bed Bottom Friction. Journal of Physical Oceanography, (schedule for the March issue).

No. 83. Grumbine, R.W., 1993: Notes and Correspondence A Sea Ice Albedo Experiment with the NMC Meduim Range Forecast Model. Weather and Forecasting, (submitted).

No. 84. Chao, Y.Y., 1993: The Gulf of Alaska Regional Wave Model. Technical Procedure Bulletin.

No. 85. Chao, Y.Y., 1993: Implementation and Evaluation of the Gulf of Alaska Regional Wave Model. OPC Office Note, 35 pp.


DEPARTMENT OF COMMERCE
UNITED STATES OF AMERICA